Model-based assessment of

geophysical observations

Gilda Currenti

Istituto Nazionale di Geofisica e Vulcanologia, Osservatorio Etneo

28-31 may 2024 – Potsdam

Osservatorio Etneo

Istituto Nazionale di Geofisica e Vulcanologia

Quantitative model-based assessment of geophysical observations

Displacement

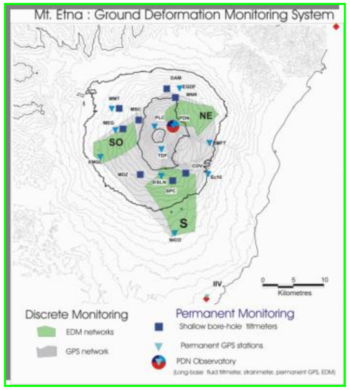

Borehole

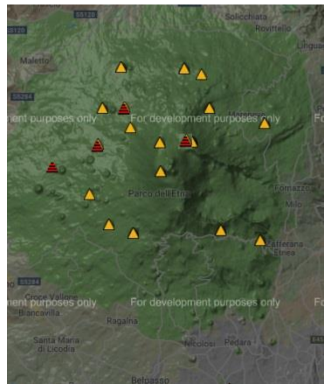

DInSAR

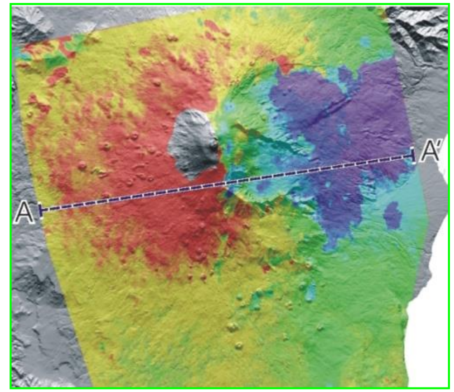

Potential Field

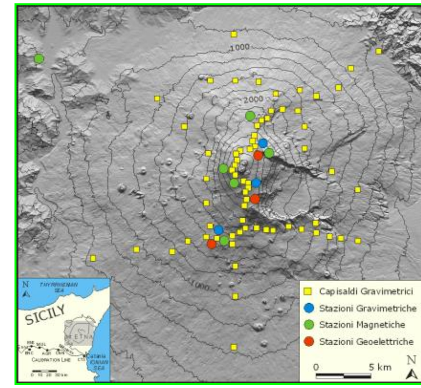

Elaborated inverse methods combine forward models with appropriate algorithms to find the best parameter set that minimizes the misfit between the model values and the observations by means of an objective function. That turns the inversion problem in an optimization problem. The goal of modelling is to determine the volcanic source parameters from available observations.

Inverse Methods → **Active volcanic source**

Mathematical Model → **Inverse Methods**

Osservatorio Etneo

Gravity-heigth changes in volcanic areas

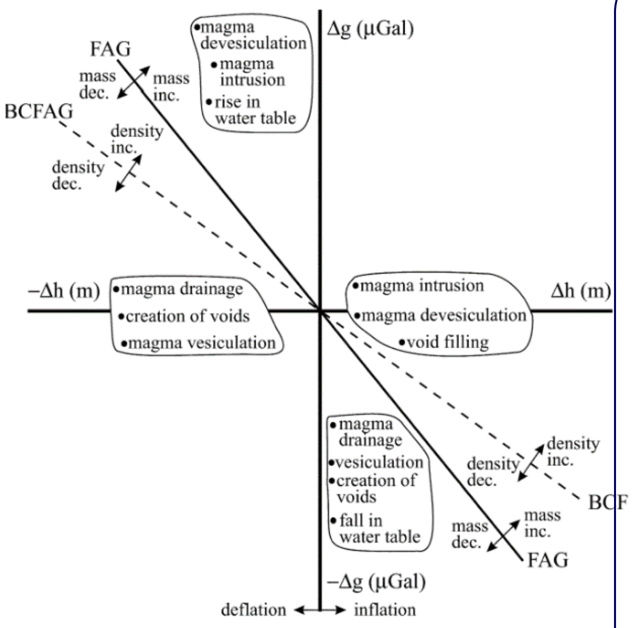

$$\frac{\delta g}{\delta h} = -\gamma + \frac{4}{3}\pi G \rho_m$$

γ=3.086 μGal/cm

The evolution of the gravity-height changes is suggested as a signature of the nature of the deformation/gravity source as a volcano moves from a rest to unrest state.

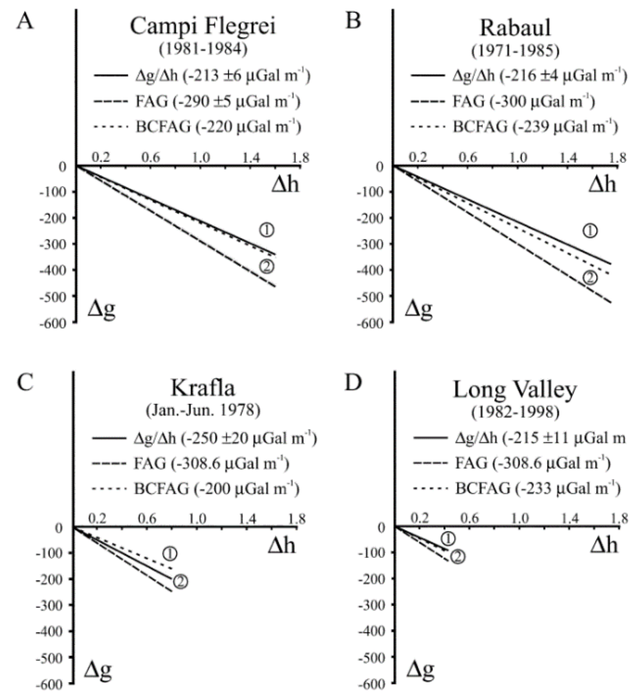

Williams & Rymer, 2000

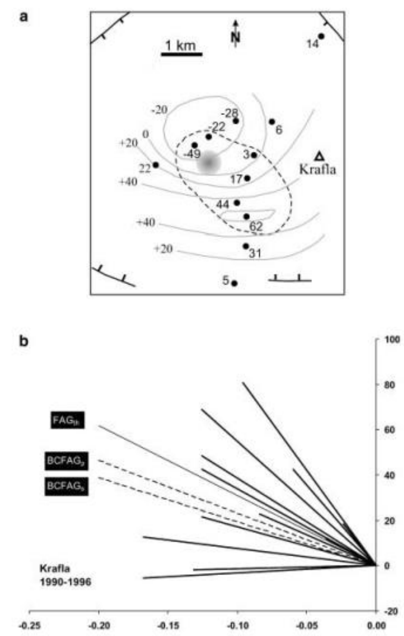

Gottsmann and Rymer, 2002

Gravity-heigth changes in volcanic areas

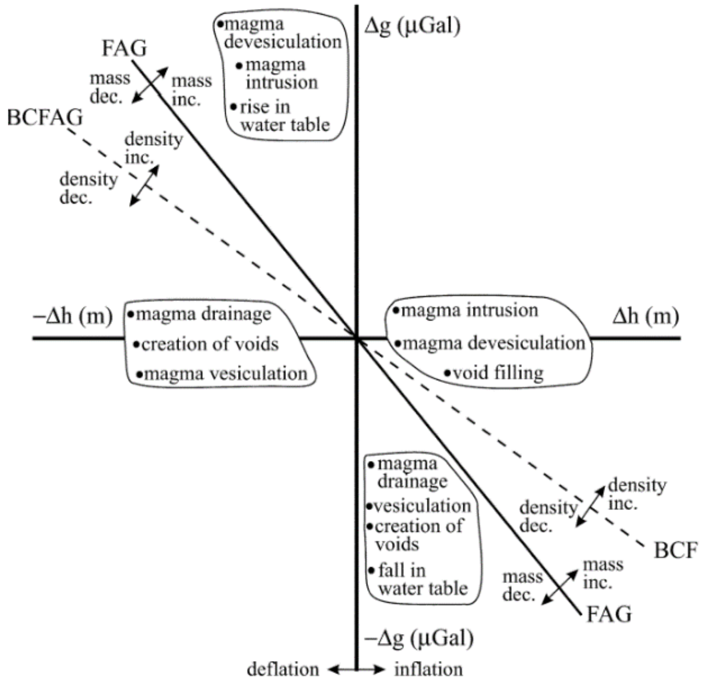

$$\frac{\delta g}{\delta h} = -\gamma + \frac{4}{3}\pi G \rho_m$$

Gravity-height changes due to either uplift or subsidence have been usually explained by the well-known Mogi model.

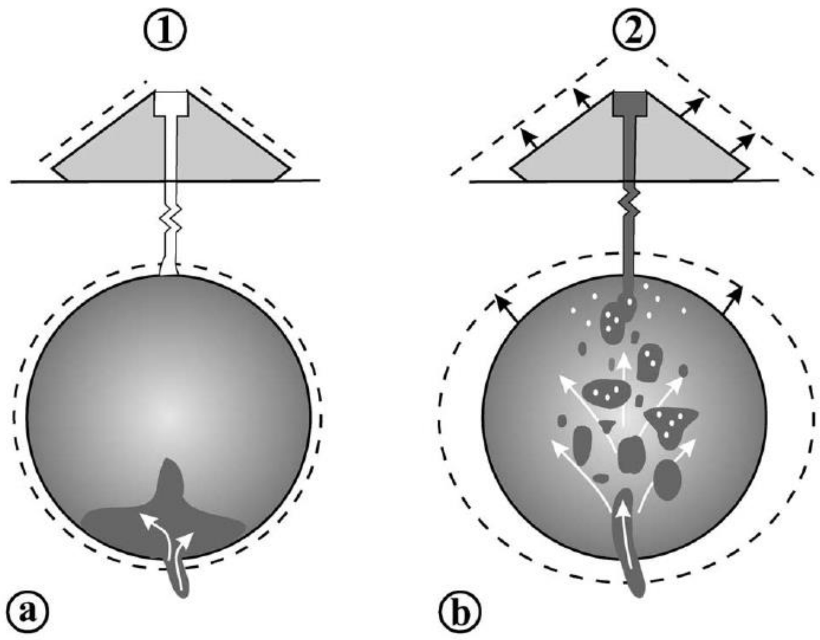

Model (1) depicts the intrusion of a magma with little or no interaction with the surrounding magma.

Model (2) represents the case when the intruding magma interacts vigorously with the surrounding magma, resulting in heating, convection, vesiculation and expansion of the reservoir.

Expected gravity variation in volcanic area

Deformation modelling

$$\nabla \cdot \boldsymbol{\sigma} = 0$$

$$\boldsymbol{\sigma} = \lambda tr(\boldsymbol{\varepsilon})\boldsymbol{I} + 2\mu\boldsymbol{\varepsilon}$$

$$\boldsymbol{\varepsilon} = \frac{1}{2}\left(\nabla \boldsymbol{u} + (\nabla \boldsymbol{u})^T\right)$$

Deformation fields

Poisson equation

$$\nabla^2 \phi_g = -4\pi G \Delta\rho(x,y,z)$$

$$\Delta g(x,y,z) = -\left(\frac{\partial \phi_g}{\partial z}\right) + \gamma_{FA} u_z$$

Gravity field

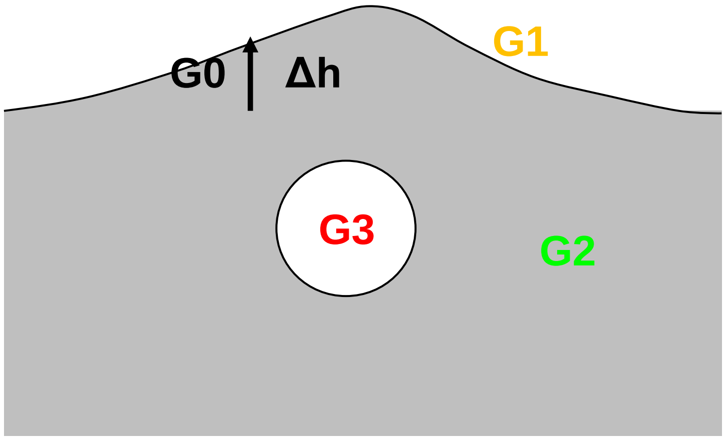

Bonafede and Mazzanti, GJI 1997

From mass conservation law: $\nabla \bullet (\rho u) = \cos t$

mass redistrbution: G_3

compressibility of surrounding medium: G_2

$$\Delta\rho(x,y,z) = \rho_m - \rho_0 \nabla \cdot \mathrm{u} - \mathrm{u} \cdot \nabla \rho_0$$

displacement of density boundary: G_1

|G0| >> |G1| > |G2| > |G3| gas filled
|G0| >> |G1| > |G3| > |G2| magma filled

Gravity changes from spherical source

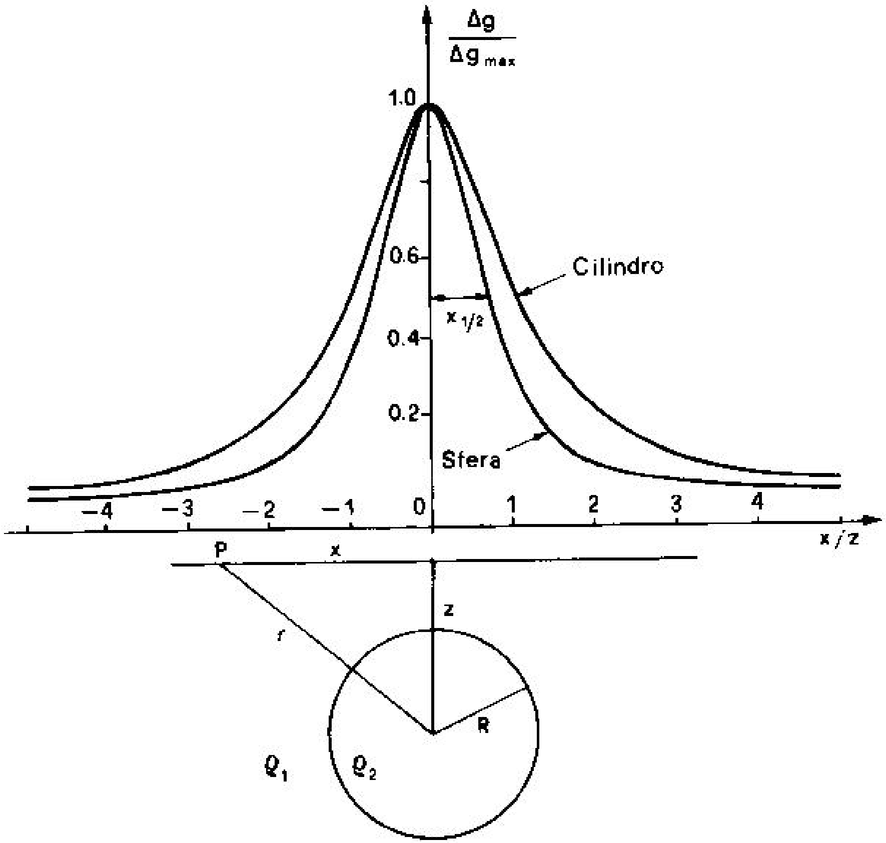

Sphere Source

$$g_z(x,y,z)=\frac{4}{3}\pi R^3\Delta\rho G\,\frac{z}{r^3}$$

$$z_c = 1.305\,x_{1/2}$$

Horizontal Cilinder Source

$$g_z(x,y,z)=2\pi G\,\frac{\Delta\rho a^2}{z}\,\frac{1}{\left(1+\frac{x^2}{z^2}\right)}$$

$$z_c = x_{1/2}$$

Analytical Solutions

$$\delta g_1 = 2\pi G \rho_0 \delta h$$

$$\delta g_2 = G\left[(\rho' - \rho_0)\Delta V\right]\frac{z}{z^2 + r^2} = \frac{4}{3}\pi(\rho' - \rho_0)G\delta h$$

$$\delta g_3 = -\frac{2}{3}\pi G \rho_0 \delta h$$

Hagiwara, 1977

without addition of new mass (V'ρ'=Vρ)

$$\delta g_2 = -\frac{4}{3}\pi G \rho_0 \delta h = -G\rho_0 \Delta V \frac{z}{z^2 + r^2}$$

$$\delta g_1 + \delta g_2 + \delta g_3 = 0$$

without addition of new mass (ρ')

$$\delta g_2 = \frac{4}{3}\pi G \rho' \delta h = G\rho' \Delta V \frac{z}{z^2 + r^2}$$

$$\delta g = \delta g_1 + \delta g_2 + \delta g_3 = \frac{4}{3}\pi G \rho' \delta h$$

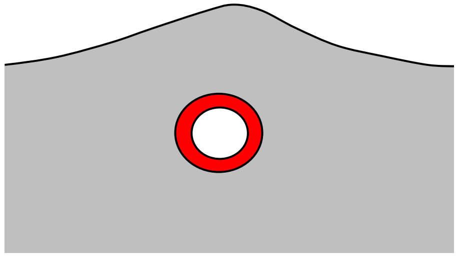

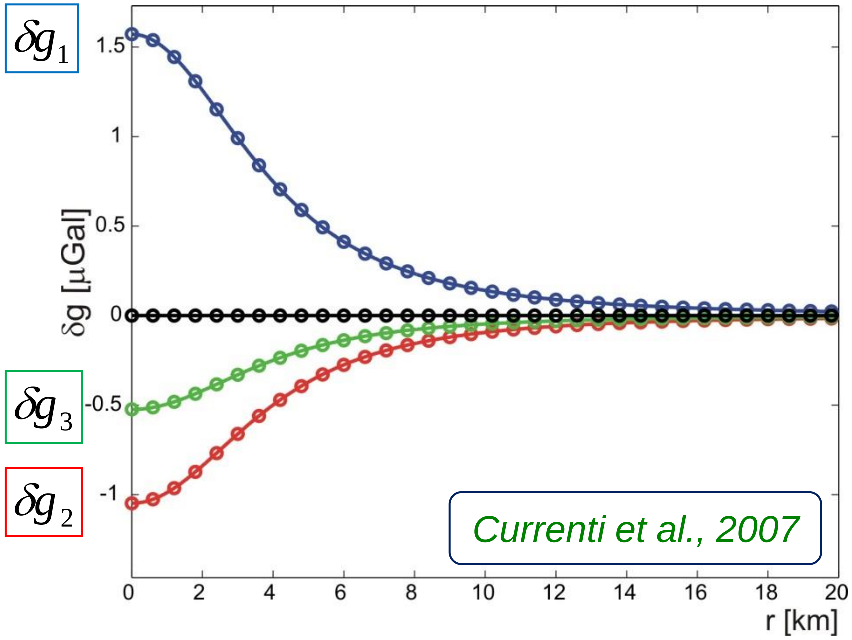

Currenti et al., 2007

Osservatorio Etneo
Istituto Nazionale di Geofisica e Vulcanologia

Gravity-Height changes in volcanic areas

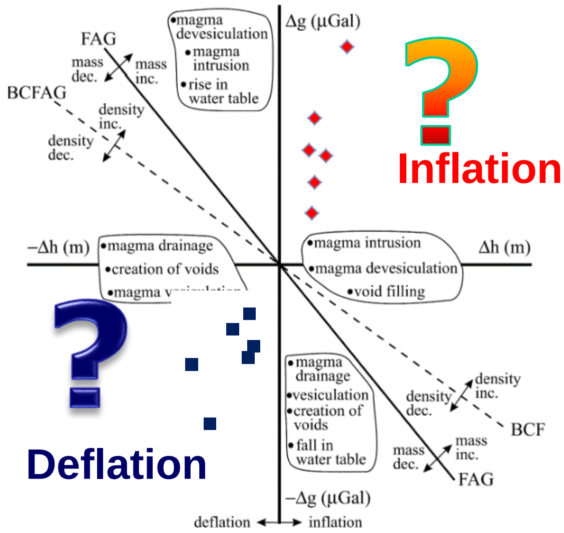

Etna volcano

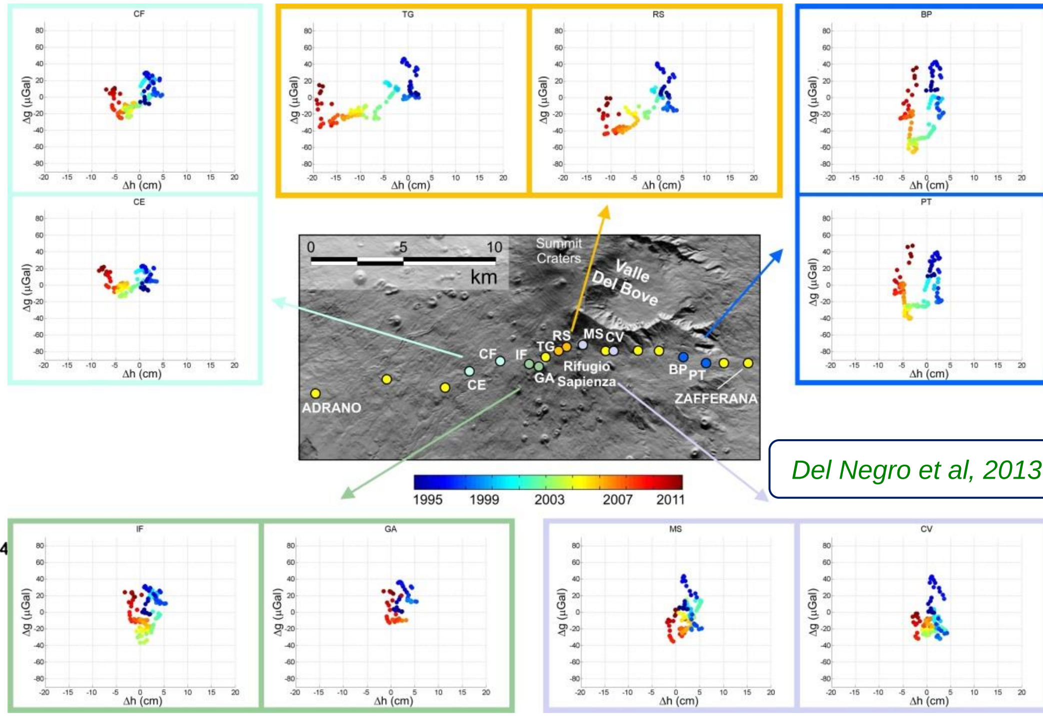

Del Negro et al, 2013

Mayon volcano

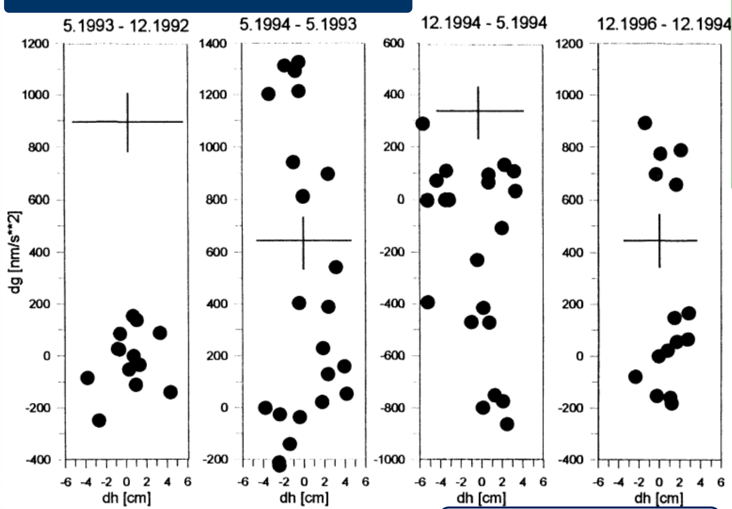

Jentzsch et al, 2000

Mogi model often appears at odds with geology of the volcanoes, geometry of chamber and properties of the magmatic fluids. When modeling gravity-height changes, it is important to properly take into account the volume change, which accommodates the input of fresh magma.

Osservatorio Etneo

Heterogeneity and Source Geometry

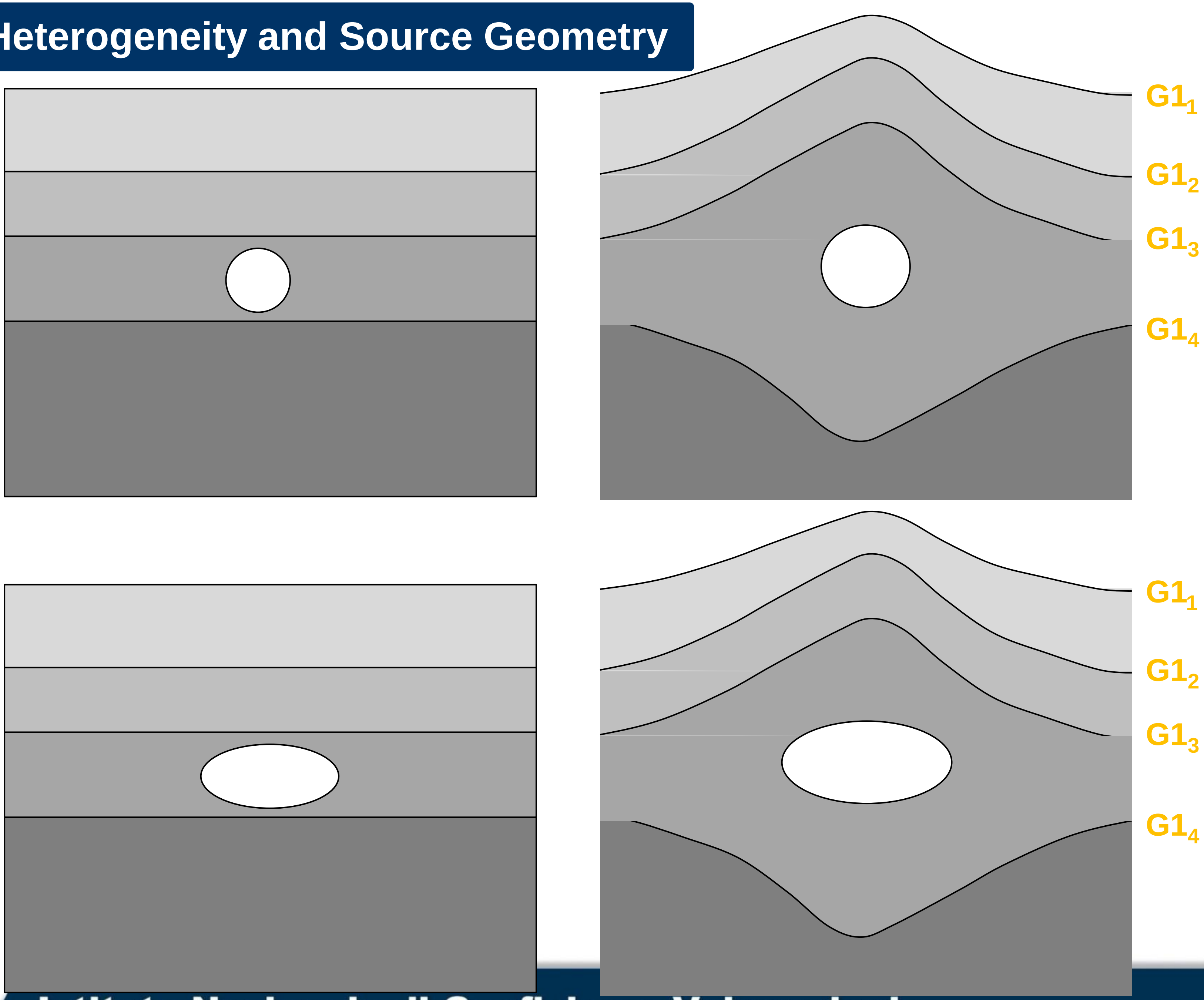

Osservatorio Etneo
Istituto Nazionale di Geofisica e Vulcanologia

Numerical Model

Deformation modelling

Numerical solutions of deformation and strain fields

Poisson equation

Gravity field

Deformation

$$\nabla \cdot \boldsymbol{\sigma} = 0$$
$$\boldsymbol{\sigma} = \lambda tr(\boldsymbol{\varepsilon})\boldsymbol{I} + 2\mu\boldsymbol{\varepsilon}$$
$$\boldsymbol{\varepsilon} = \frac{1}{2}\left(\nabla \boldsymbol{u} + (\nabla \boldsymbol{u})^T\right)$$

Gravity

$$\nabla^2\phi_g = -4\pi G\Delta\rho(x,y,z)$$
$$\Delta g(x,y,z) = -\left(\frac{\partial\phi_g}{\partial z}\right) + \gamma_{FA}u_z$$

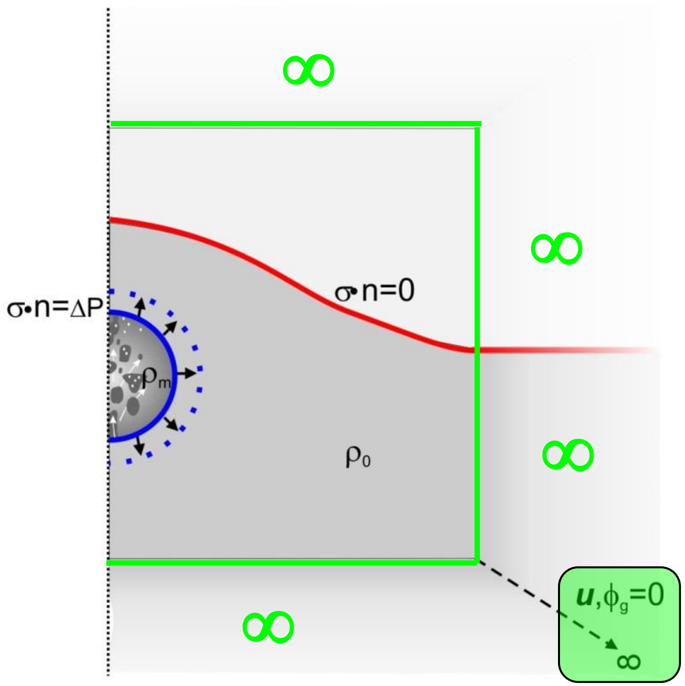

In order to solve the Poisson's equation the potential are to be assigned at the boundaries of the domain. The computational domain is a rectangle extending 30 x 30 km from the source and infinite mapped elements are added along the external boundaries. The ∞ **mapped elements** use appropriate **transformation functions to map** the finite domain into an infinite one and, hence, to make the displacements and the gravitational potential vanish toward infinity.

Osservatorio Etneo

Inflation with no mass input for ellipsoidal source

Currenti, GJI 2014

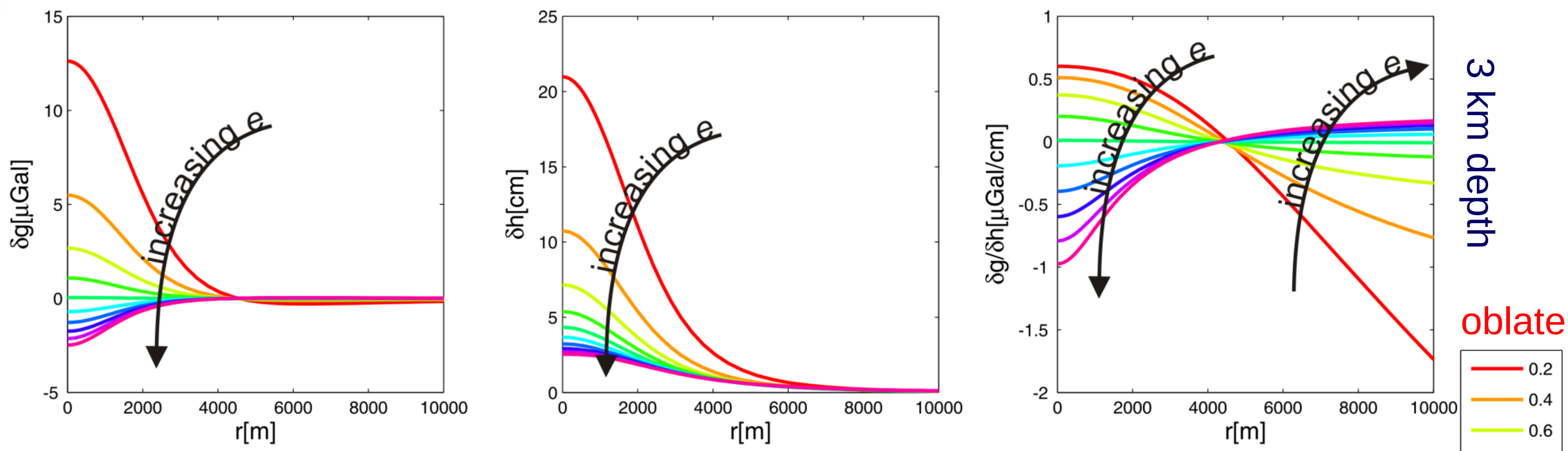

oblate

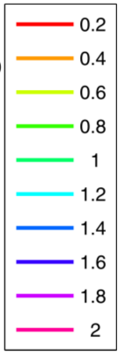

e > 1 $\delta g_1 < -\delta g_2 - \delta g_3 \rightarrow \delta g < 0$

e < 1 $\delta g_1 > -\delta g_2 - \delta g_3 \rightarrow \delta g > 0$

prolate

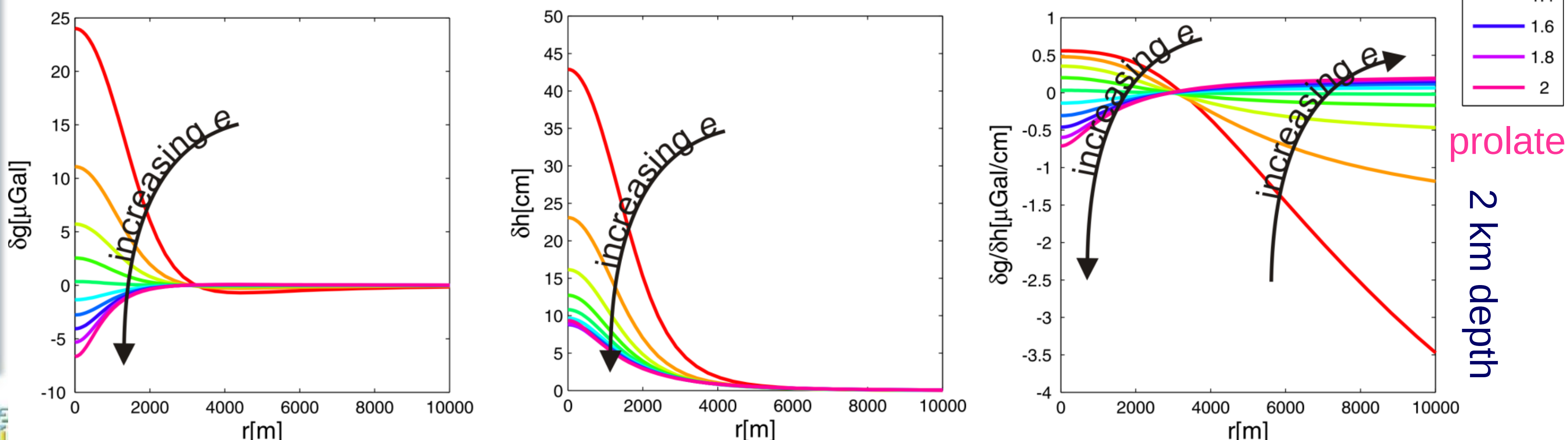

Inflation with mass input

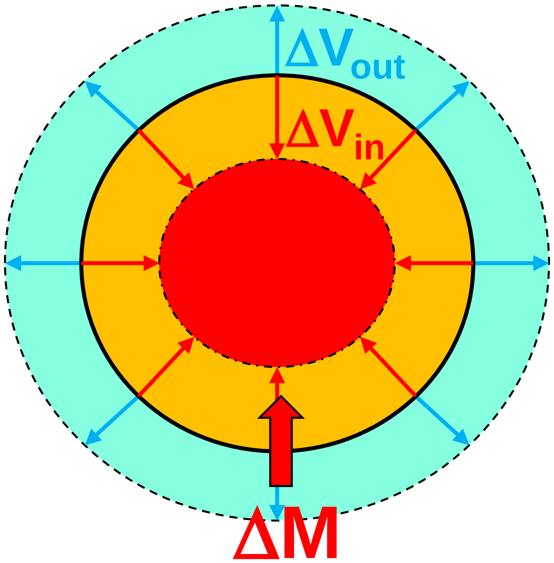

$\Delta V = \Delta V_{in} + \Delta V_{out}$

When magma chamber inflates accompanied by the entering of new fresh magma, the new mass is accommodated in the displaced volume ΔV given by two terms: ΔV_{in}, due to the contraction of the magma already resident in the chamber, and ΔV_{out}, generated by the expansion of the rocks surrounding the chamber. The source expansion ΔV_{out} is provided by the boundary condition of assigned tractions ΔP acting normally to the source boundary. It is generally assumed that the magma is subjected to the same pressure change ΔP in order to be in mechanical equilibrium with the surrounding elastic medium.

$\Delta V_{in} = -V\varepsilon_{kk}$

$\varepsilon_{kk} = -3\Delta R/R = \Delta P\chi$

relative contraction $\Delta V_{in}/V$ is independent of ellipsoid aspect ratios

Magma compressibility is controlled by magma chamber conditions (i.e., pressure, gas volume fraction, phenocryst content, temperature, and depth) and is very small for a gas-free magma (0.04-0.2 GPa^{-1}; *Spera, 2000*) but is relatively large if volatiles exsolve reaching up to 10 GPa^{-1} for basaltic magma or more for felsic magma (*Rivalta and Segall, 2008; Rivalta, 2010*).

Osservatorio Etneo

Geometry effect

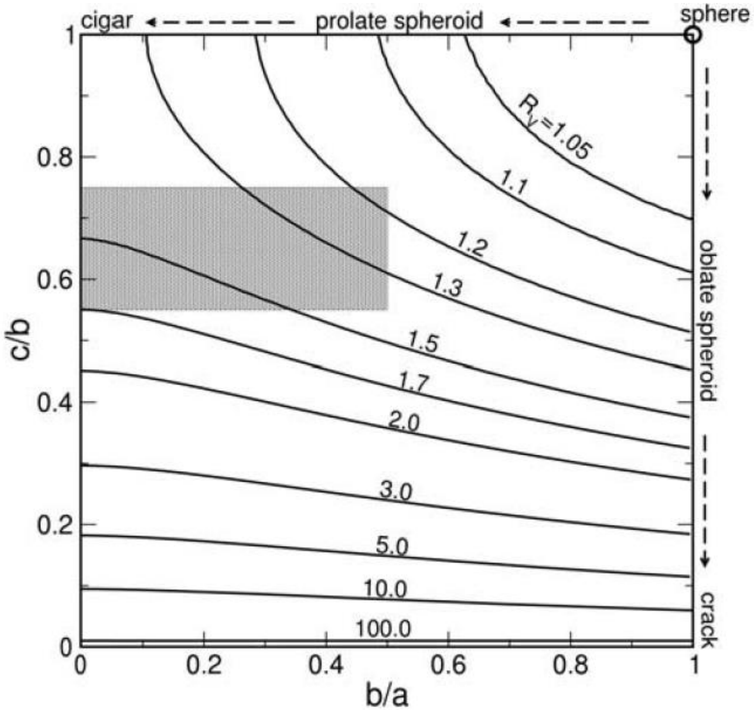

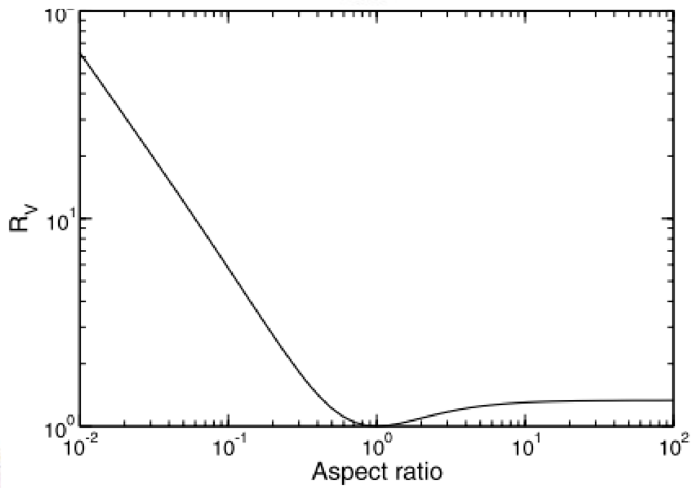

The expansion ΔV_{out} of the source wall depends on the effective chamber compressibility β_c:

$$\Delta V_{out} = \beta_c \Delta P V$$

For a spherical magma chamber

$$\beta_c = 3/4\mu$$

and hence:

$$\Delta V_{out} = 3\Delta P V/(4\mu)$$

In general

$$R_v = \Delta V_{out}^{el} / \Delta V_{out}^{sp} > 1$$

At constant pressure and initial volume an ellipsoidal source may accommodate more mass than a spherical one.

Amoruso & Crescentini 2009

PROLATE

$$\Delta V \approx \frac{2\, b^2 \pi\, \Delta P}{3\,\mu}\left(a_1\left(a \log\left(\frac{a-c}{a+c}\right)(-1+2\,\nu) + c\,(-5+4\,\nu)\right) - 2\,c^3\, b_1\right)$$

Cervelli, USGS 2013

$$\Delta V \approx \cancel{\frac{\Delta P\, b^2 \pi a}{\mu}}$$

Tiampo et al, JVGR 2000

Numerical Model

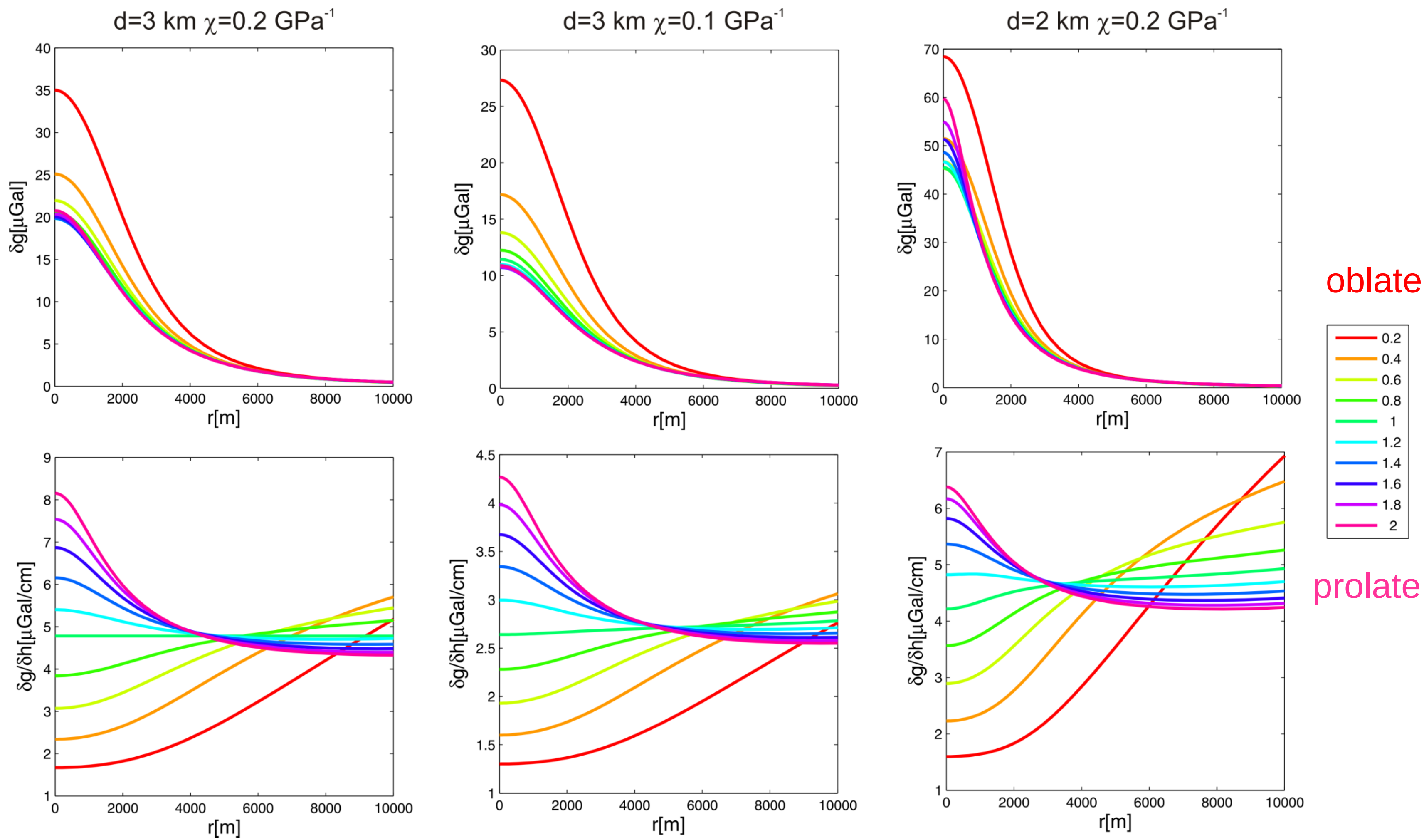

The numerical result for the deeper (3 km) spherical source (***e=1***) agrees with the analytical solution (*Bonafede & Ferrari 2009*)

$$\frac{\delta g}{\delta h} = \frac{4}{3}\pi G \rho_m \left(1 + \frac{4}{3}\mu\chi\right)$$

Osservatorio Etneo

Application to Etna

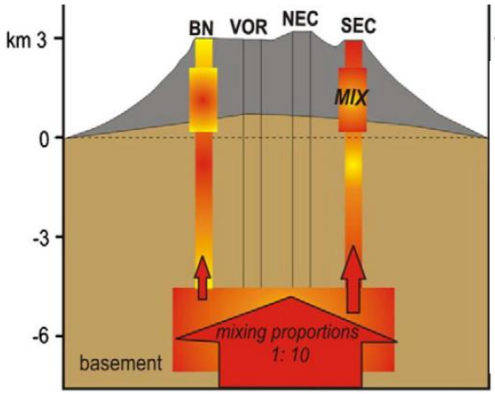

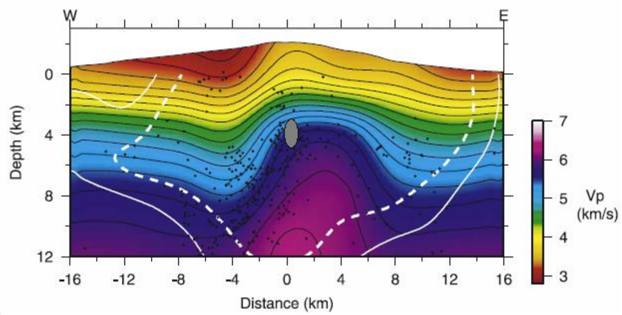

The heterogeneous structure of Etna plays a significant role in the predictions of gravity and deformation fields induced by pressurized sources. The geometry of the numerical model is defined on the basis of stratigraphical constraints, seismic tomography and gravity prospecting.

Geodetic and petrologic investigations have highlighted a multifaceted Etna's plumbing system consisting mainly of 2 storage regions, where magma ascending from depth accumulates undergoing various magmatic processes, mainly fractional crystallization and mixing: (i) a deeper region between 2-6 km b.s.l. and (ii) an upper one above 1 km a.s.l.

	Volcanites VE	Flysh FL	Carbonates HP	Dyke complex DC
Density (kg m^{-3})	2500	2600	2700	3000
Young modulus (GPa)	30	16.5	35	50
Poisson ratio	0.2	0.3	0.25	0.25

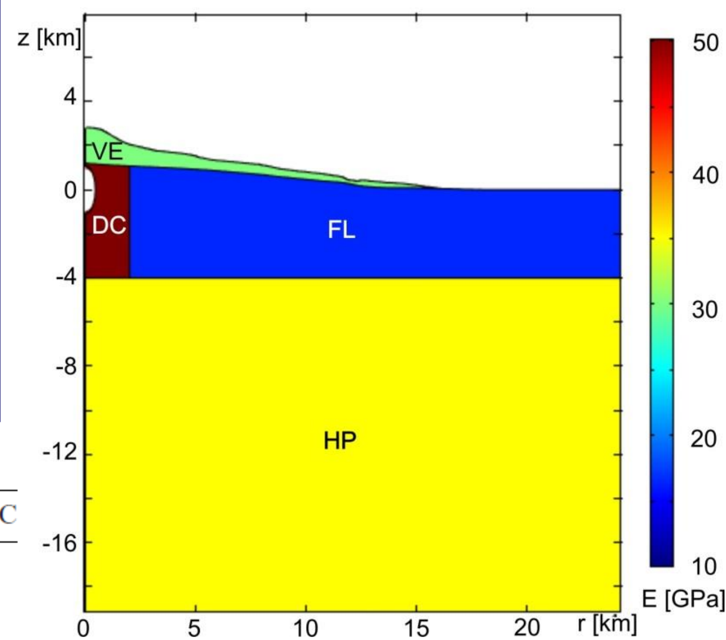

Osservatorio Etneo

1994-1995 inflation period at Etna

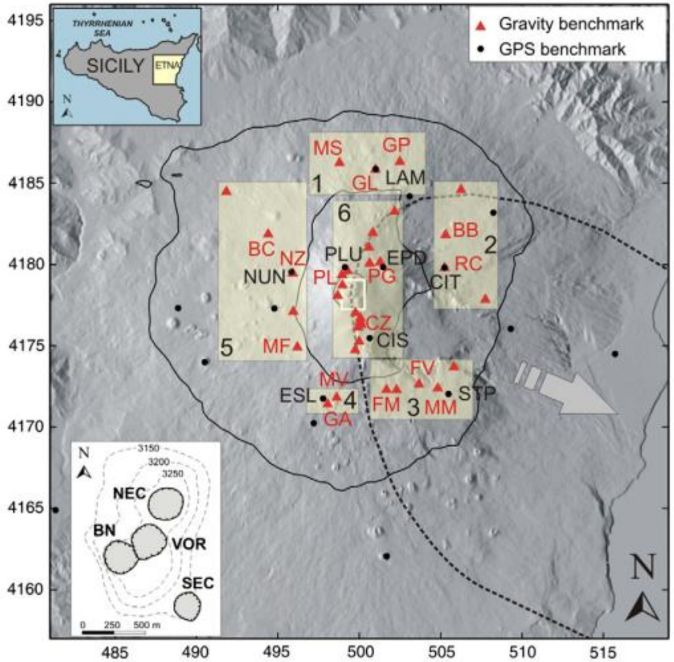

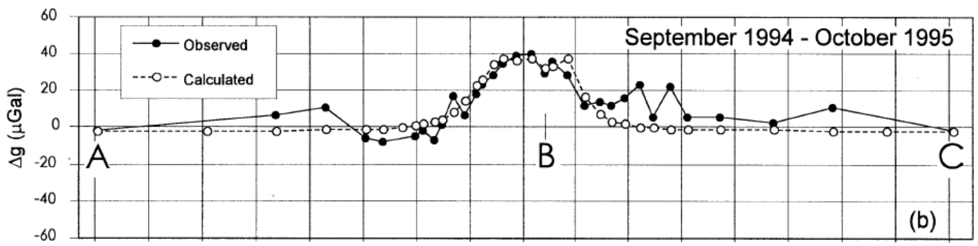

Budetta et al, GJI 1999

The model predictions are compared with the observations carried out at Etna during the 1994-95 inflation period. Gravity measurements revealed mainly a positive change of about 40 μGal accompanied by negligible uplifts within 5 cm. A prolate ellipsoid (e = 2) points to an accumulation of 1.45×10^{10} kg simulating shallow conduit processes.

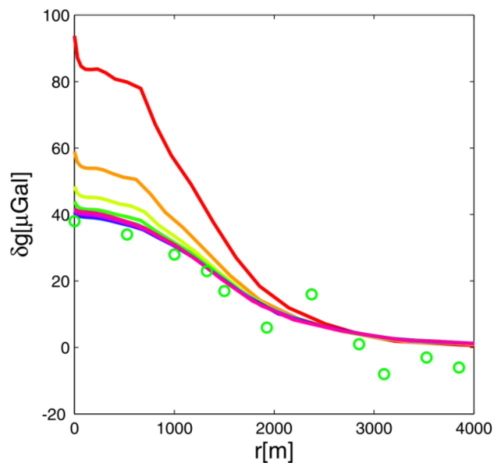

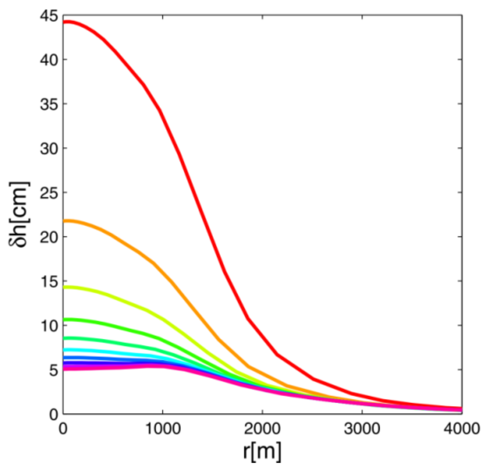

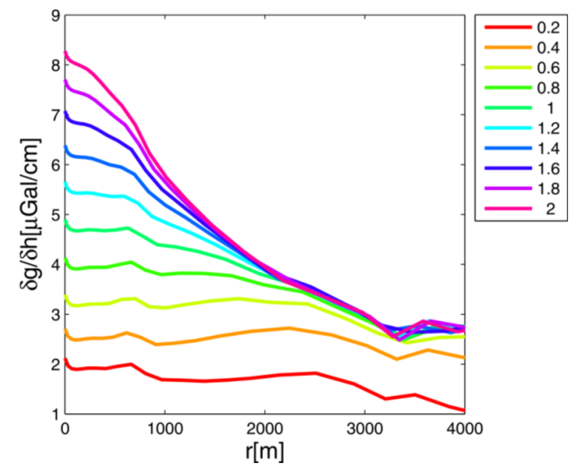

Osservatorio Etneo

Expected gravity variation in volcanic area

Deformation modelling

$$\nabla \cdot \boldsymbol{\sigma} = 0$$
$$\boldsymbol{\sigma} = \lambda tr(\boldsymbol{\varepsilon})\boldsymbol{I} + 2\mu\boldsymbol{\varepsilon}$$
$$\boldsymbol{\varepsilon} = \frac{1}{2}\left(\nabla \boldsymbol{u} + (\nabla \boldsymbol{u})^T\right)$$

Deformation/Strain fields

Poisson equation

$$\nabla^2 \phi_g = -4\pi G \Delta\rho(x,y,z)$$
$$\Delta g(x,y,z) = -\left(\frac{\partial \phi_g}{\partial z}\right) + \gamma_{FA} u_z$$

Gravity field

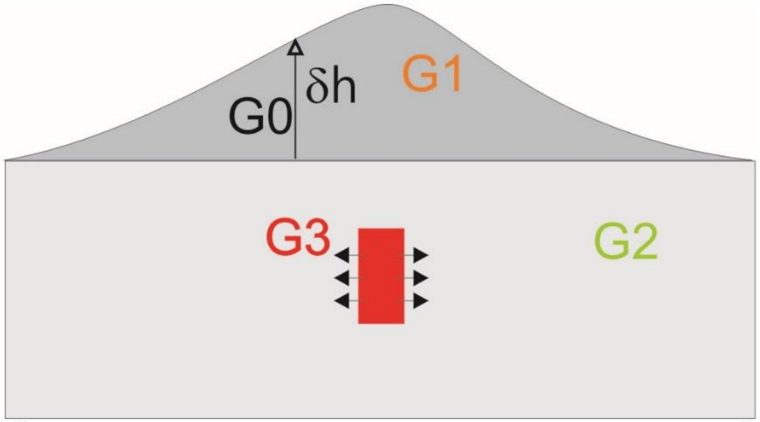

Gravity changes cannot be interpreted only in terms of additional mass input at some depth without taking into account the deformation of the surrounding rock required to host the magma volume. From mass conservation law it follows that:

mass redistrbution: G_3

compressibility of surrounding medium: G_2

$$\Delta\rho(x,y,z) = \rho_m - \rho_0 \nabla \cdot \mathrm{u} - \mathrm{u} \cdot \nabla \rho_0$$

displacement of density boundary: G_1

|G0| >> |G1| > |G2| > |G3| gas filled
|G0| >> |G1| > |G3| > |G2| magma filled

Okubo model

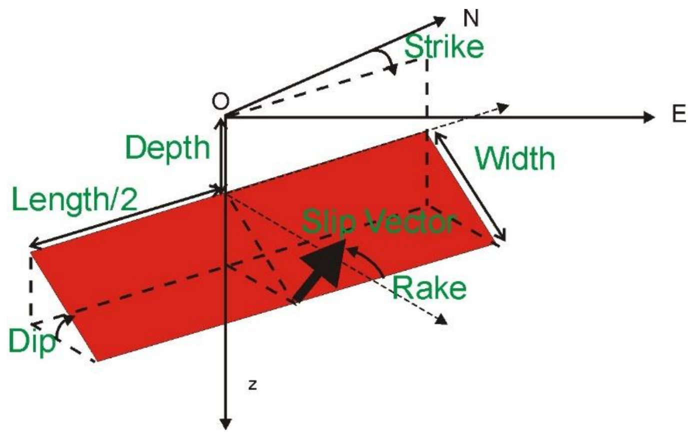

Source Parameters	Value
Length	10 km
Width	10 km
Depth	1 km
ρ_m	2670 kg/m^3
Dislocation	5 m

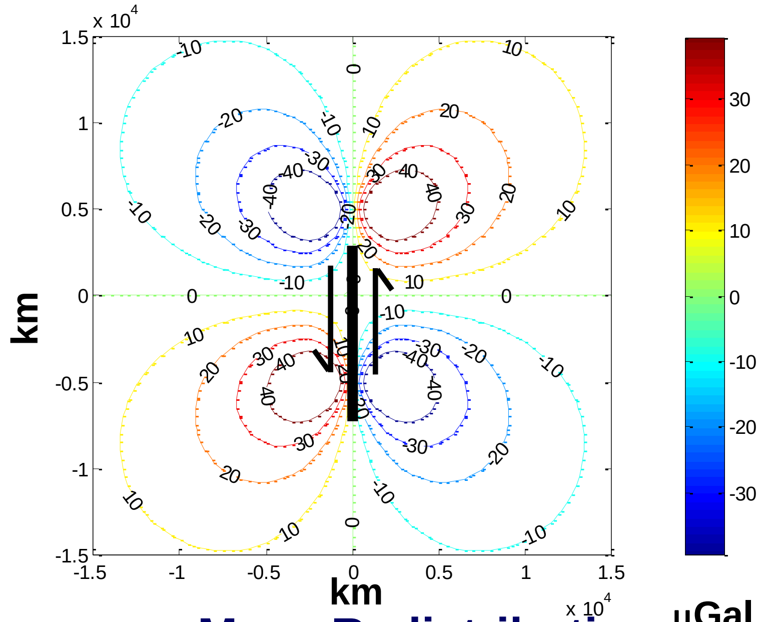

Mass Redistribution

$\delta g_1 + \delta g_3$

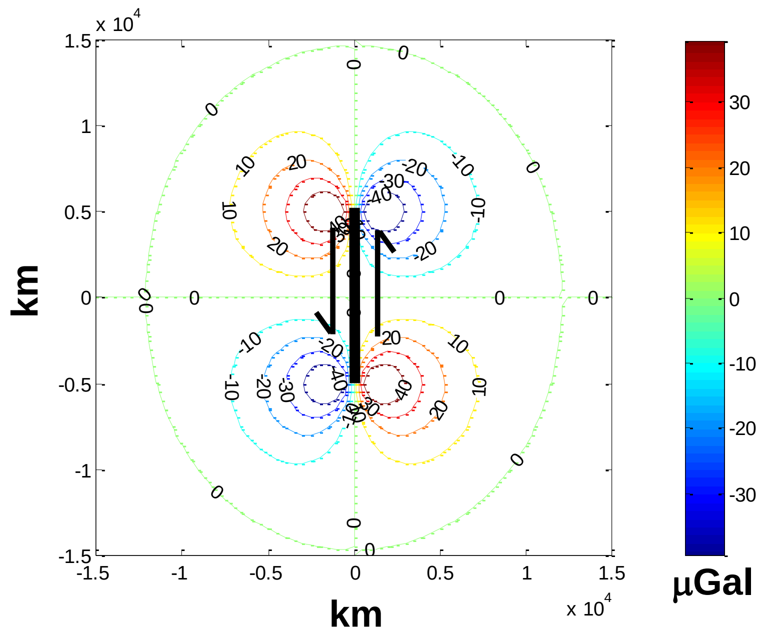

Mass Redistribution+Free Air Effect

$\delta g_1 + \delta g_3 + \delta g_0$

Tensile Opening

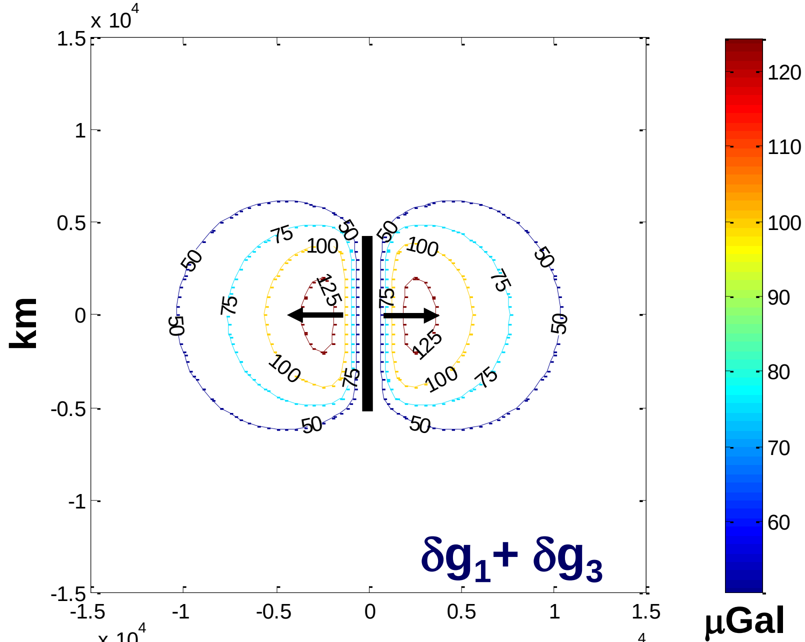

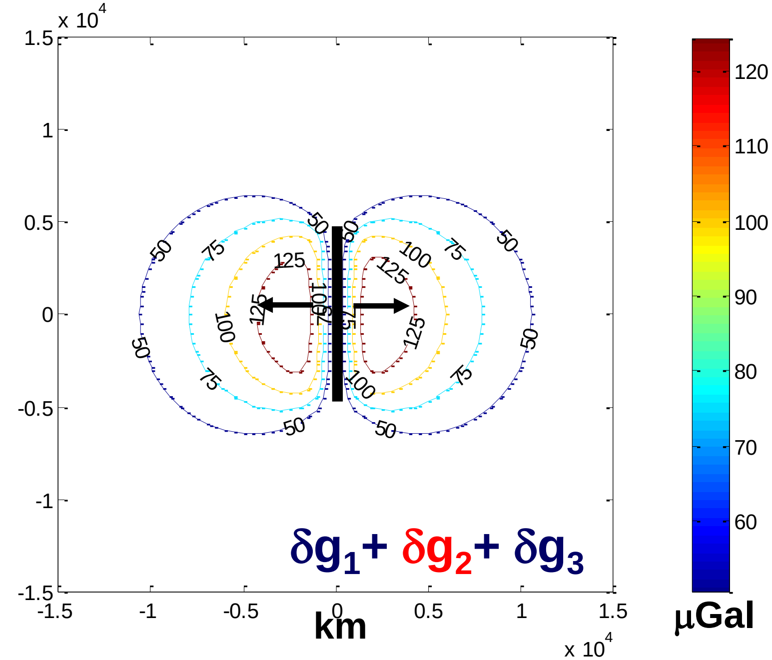

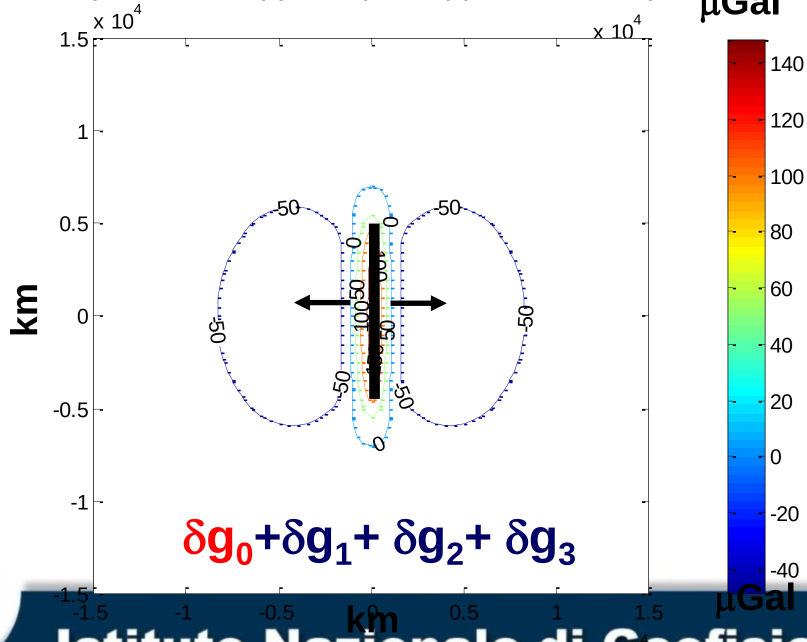

Source Parameters	Value
ρ'_m	+200 kg/m³
ρ_m	2670 kg/m³

These computations are applicable to modeling gravity contribution for both earthquake and fissure eruptions (tensile fracturing).

Magma intrusion at Usu Volcano in the 2000 eruption

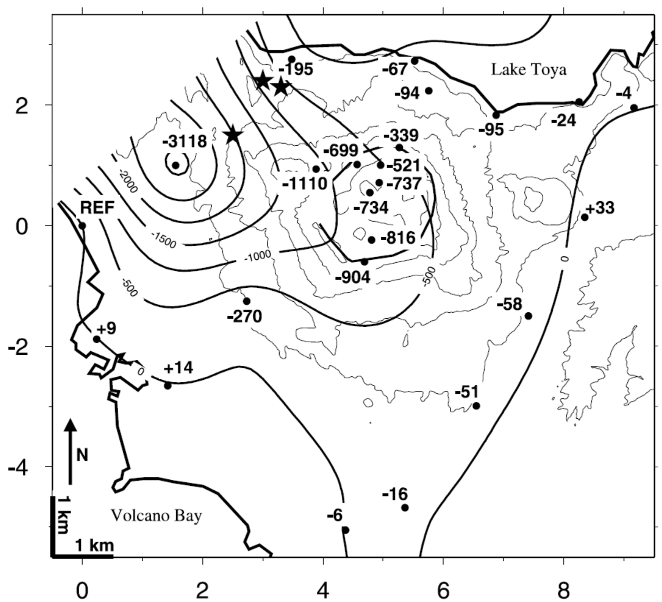

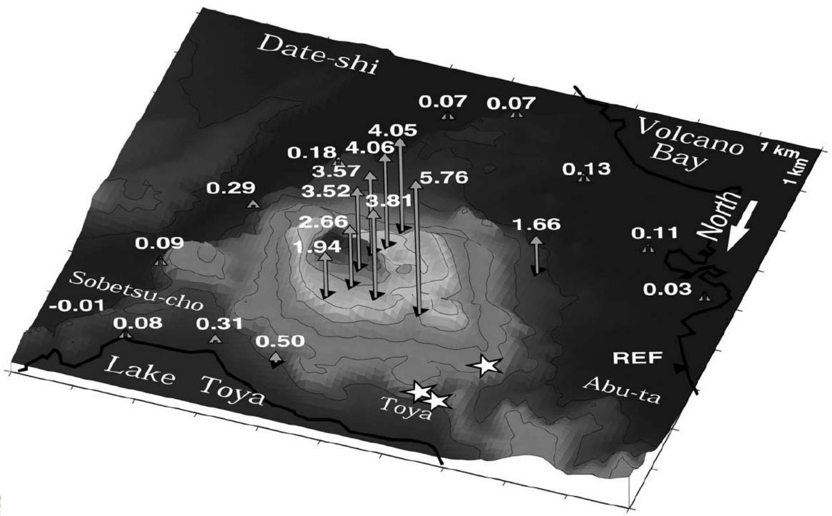

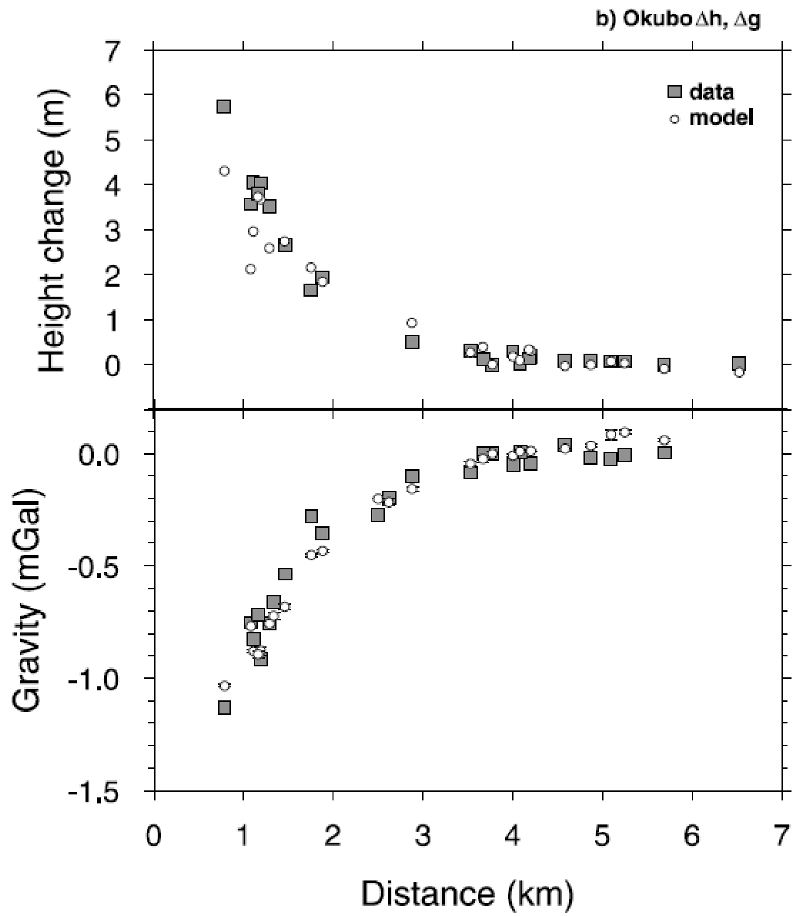

Jousset at al, JVGR 2003

Expected volcanomagnetic variation

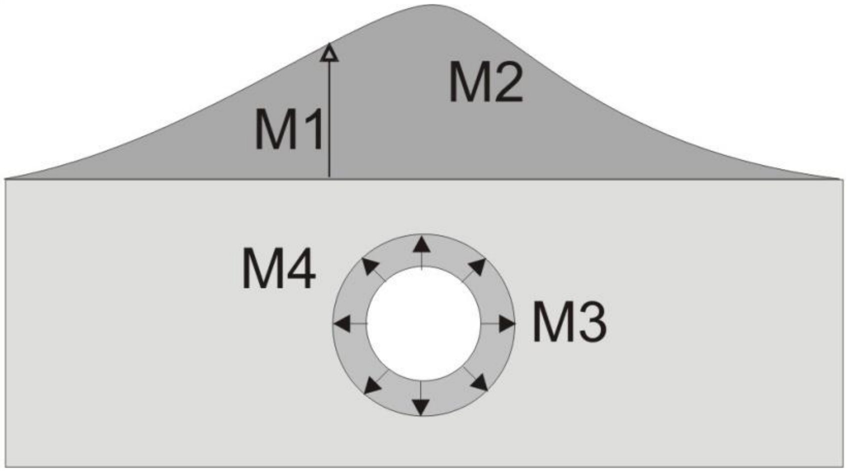

Magnetic variations can be accounted for by four contributions: (M1) "free air" magnetic effect resulting from movement of the observation site in the Earth's main field, (M2) the redistribution of magnetized mass, (M3) **thermal demagnetization** and **remagnetization** effect, (M4) change due to the **piezomagnetic** mechanism.

|**M3**| >|**M4**| >> |M2| >> |M1| (Sasai, 1991)

Piezomagnetism relates a rock's magnetic properties to an applied stress and thus is a stress-dependent geophysical property that offers a potentially effective method for stress determination.

Cauchy-Navier Equation

$$G\nabla^2\mathbf{u} + (\lambda + G)\nabla(\nabla \cdot \mathbf{u}) = 0$$

Linear piezomagnetic effect

$$\nabla^2\phi_m = 4\pi\nabla \cdot \Delta\mathbf{J}$$

$$\Delta J_{ij} = \beta\mu\left\{-\delta_{ij}\nabla \cdot \mathbf{u} + \frac{3}{2}\left(\frac{\partial u_j}{\partial x_i} + \frac{\partial u_i}{\partial x_j}\right)\right\}J_j$$

Unrest

Rest

Piezomagnetic Effect

Thermomagnetic Effect

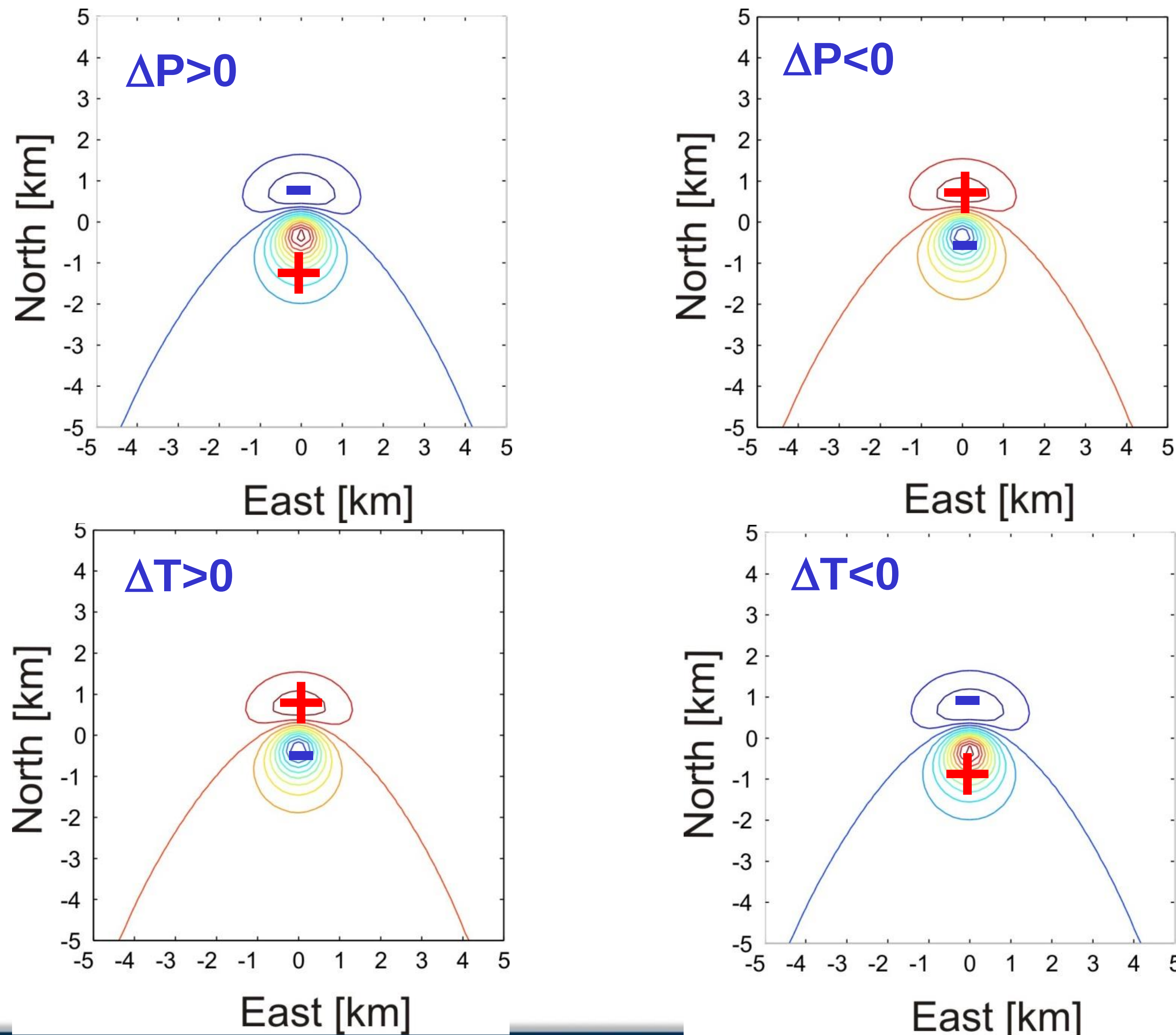

Osservatorio Etneo

GEOFIM: GEOphysical Forward/Inverse Modeling

Integrated Inversion

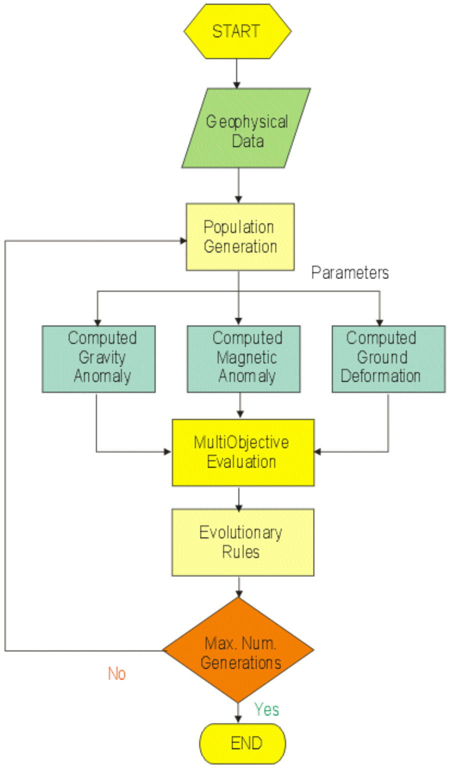

http://ufgm.ct.ingv.it/geofim/geofim.html

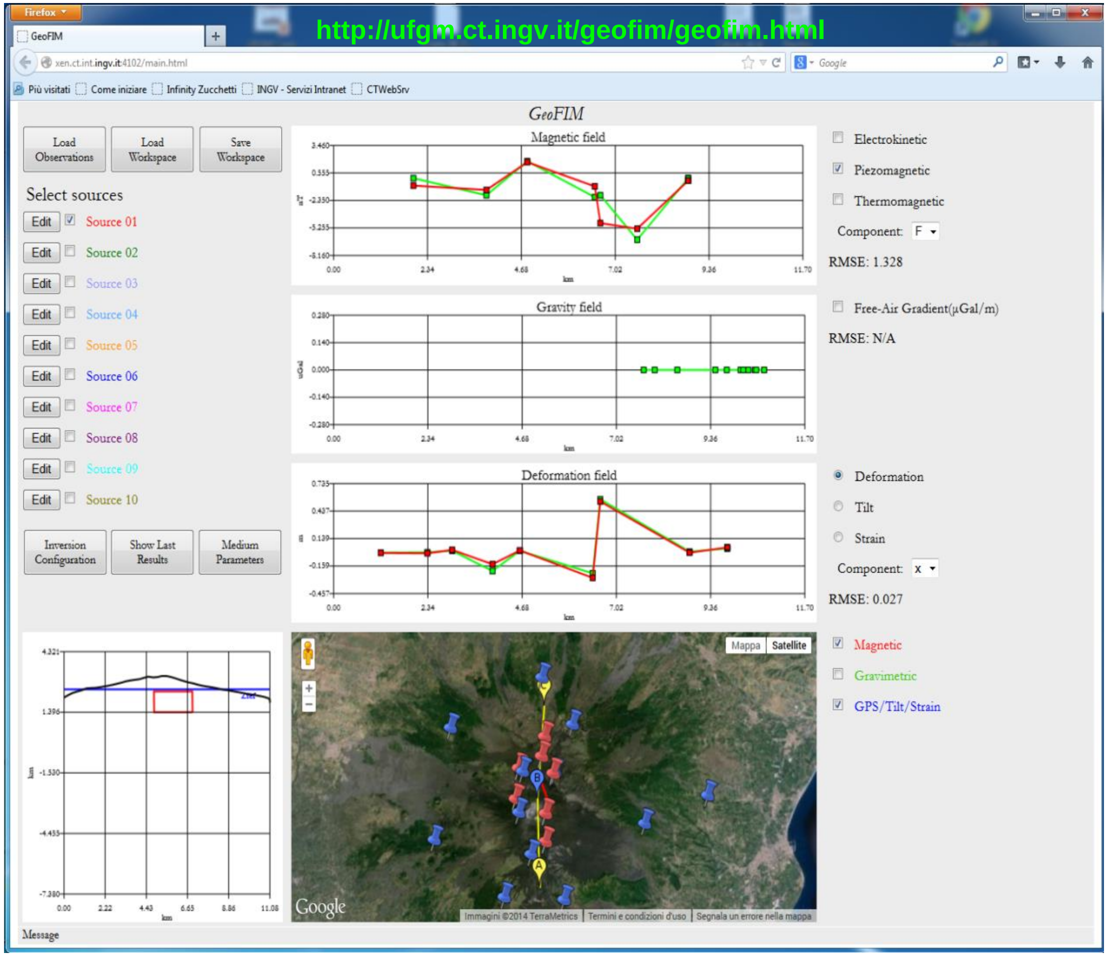

Osservatorio Etneo

Numerical Models

Despite the development of many different models, there are still discrepancies in data interpretation. This fact, together with the interest in and our need to further knowledge of all aspects of volcanic phenomena, means that more complex calculations which include effects not present in analytical models are required.

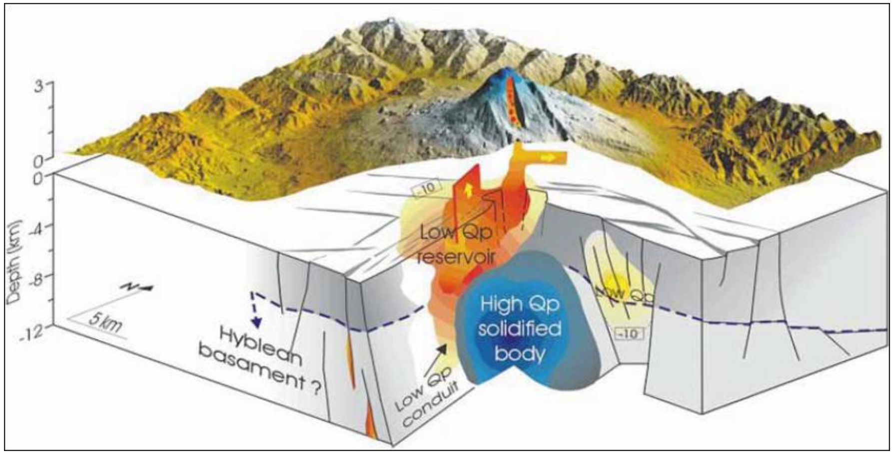

1 **Topography Effects**

2 **Elastic Heterogrneity**

3 **Rheological Properties**

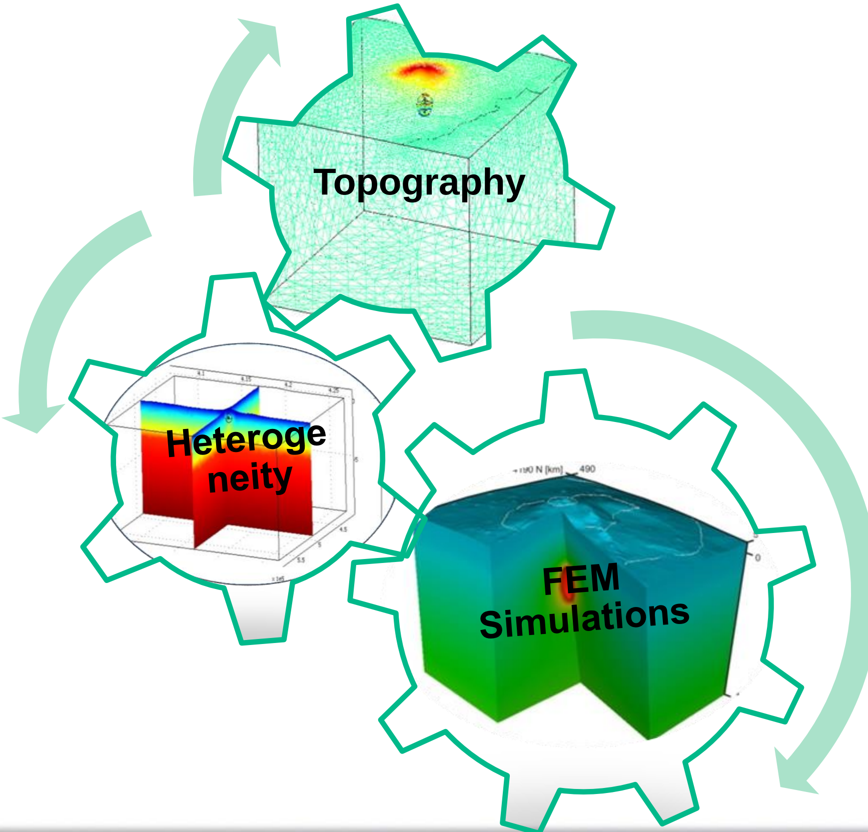

Osservatorio Etneo

Istituto Nazionale di Geofisica e Vulcanologia

Seismic Swarm

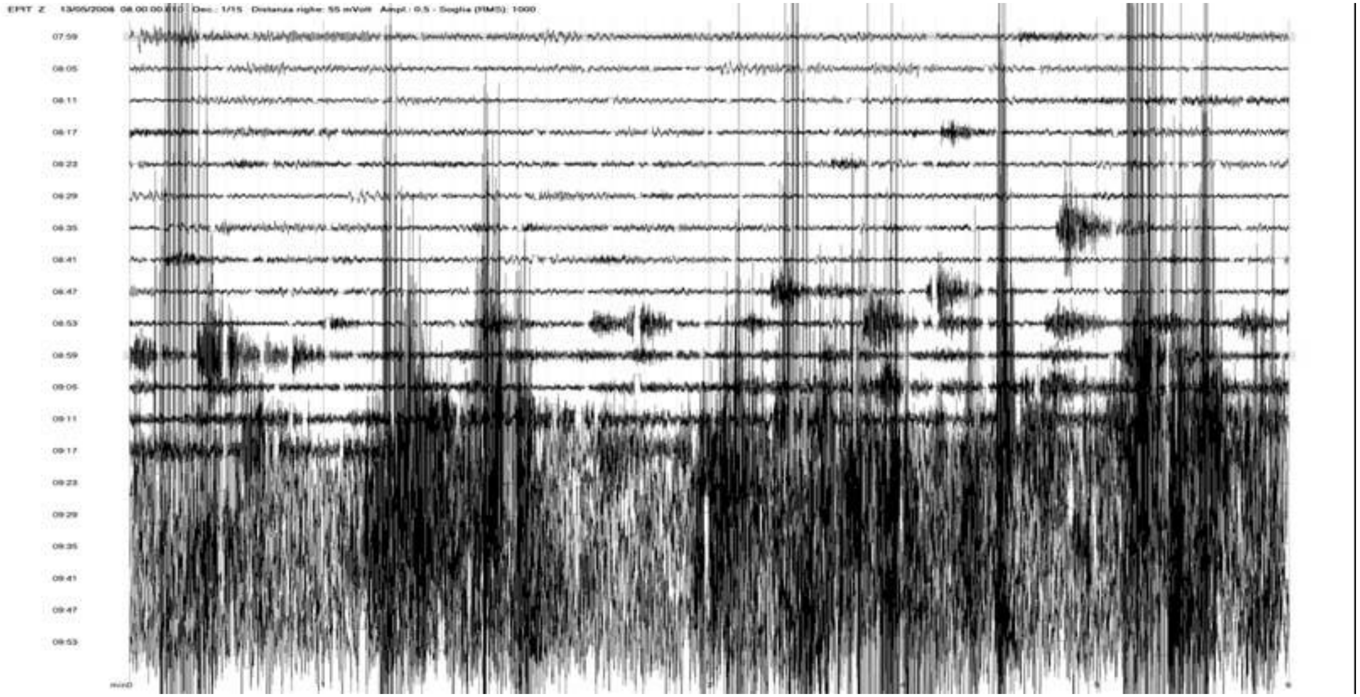

On the morning of 13th May 2008, an intense and superficial seismic swarm indicated resumption of Mt Etna eruptive activity. From 08:40 to 15:00 GMT more than 200 earthquakes, the largest being Ml 3.9, occurred in a NNW-SSE elongated area at the eastern base of Mt Etna summit craters, with hypocentral depth ranging between 1500 m b.s.l. and 1500 m a.s.l. Since 9:30 GMT a clear migration of the seismic events occurred toward the top of the NE Rift, suggesting a northward propagation of a magmatic intrusion.

Etna 2008 Eruption: Geophysical Monitoring Data

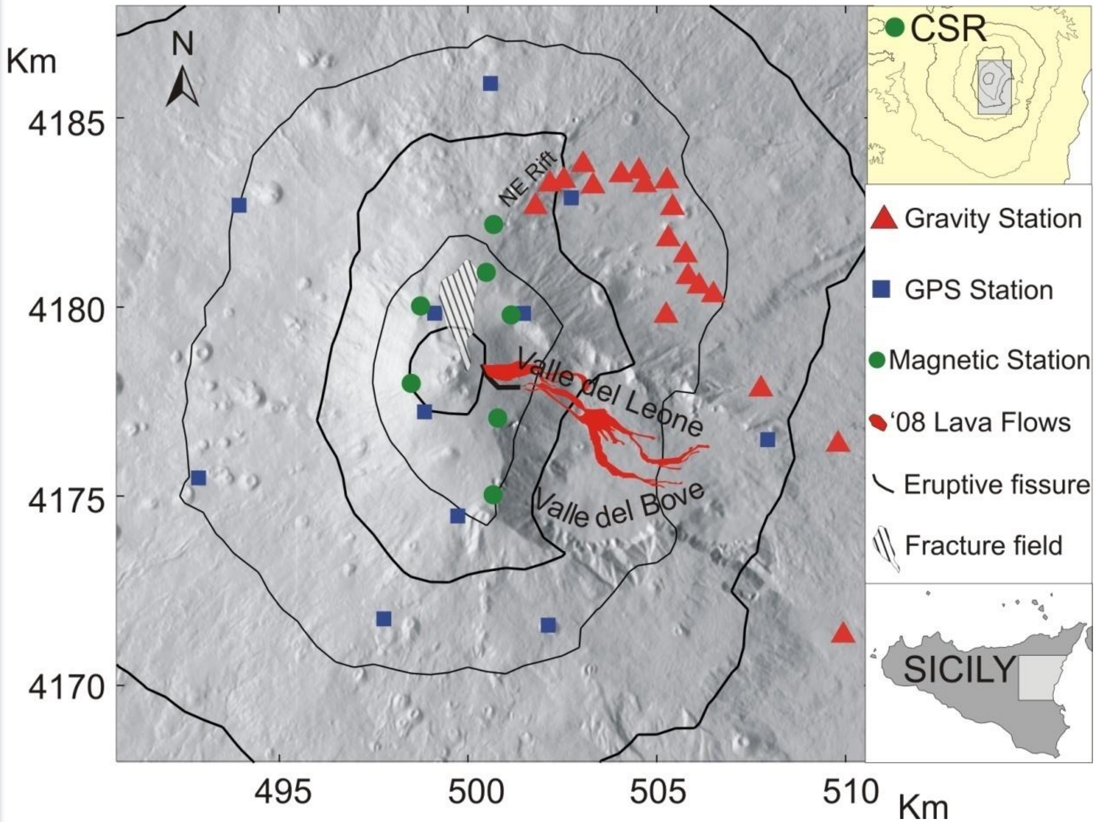

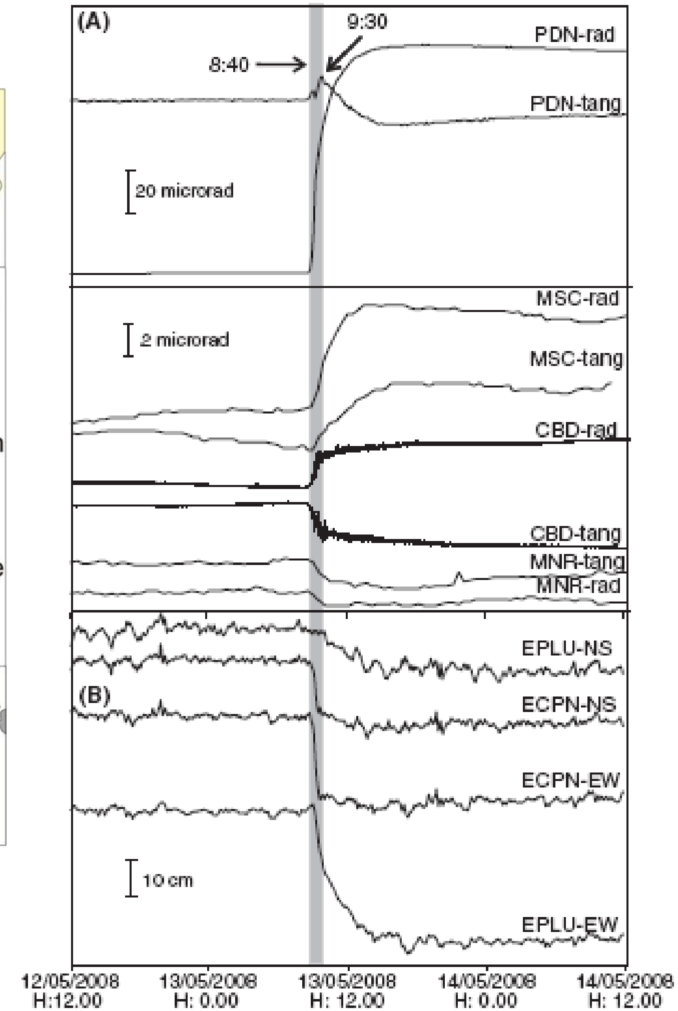

Osservatorio Etneo

10-minute means of total intensity

The magnetic data show a fast change from 09:00 to 10:00 GMT. In this time interval most of the earthquakes (about 150 of 230) were recorded.

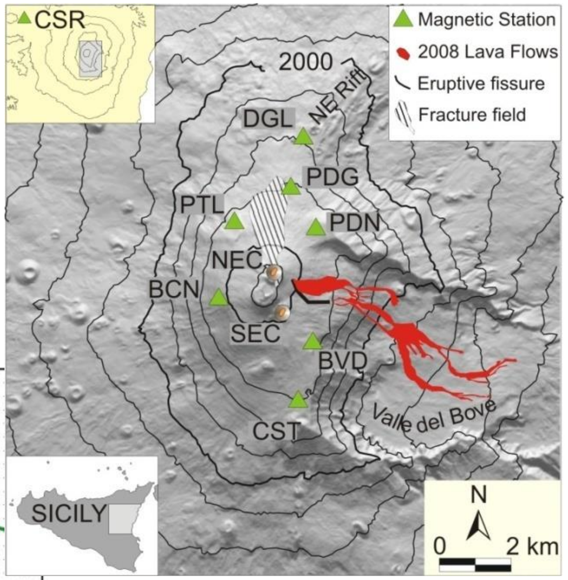

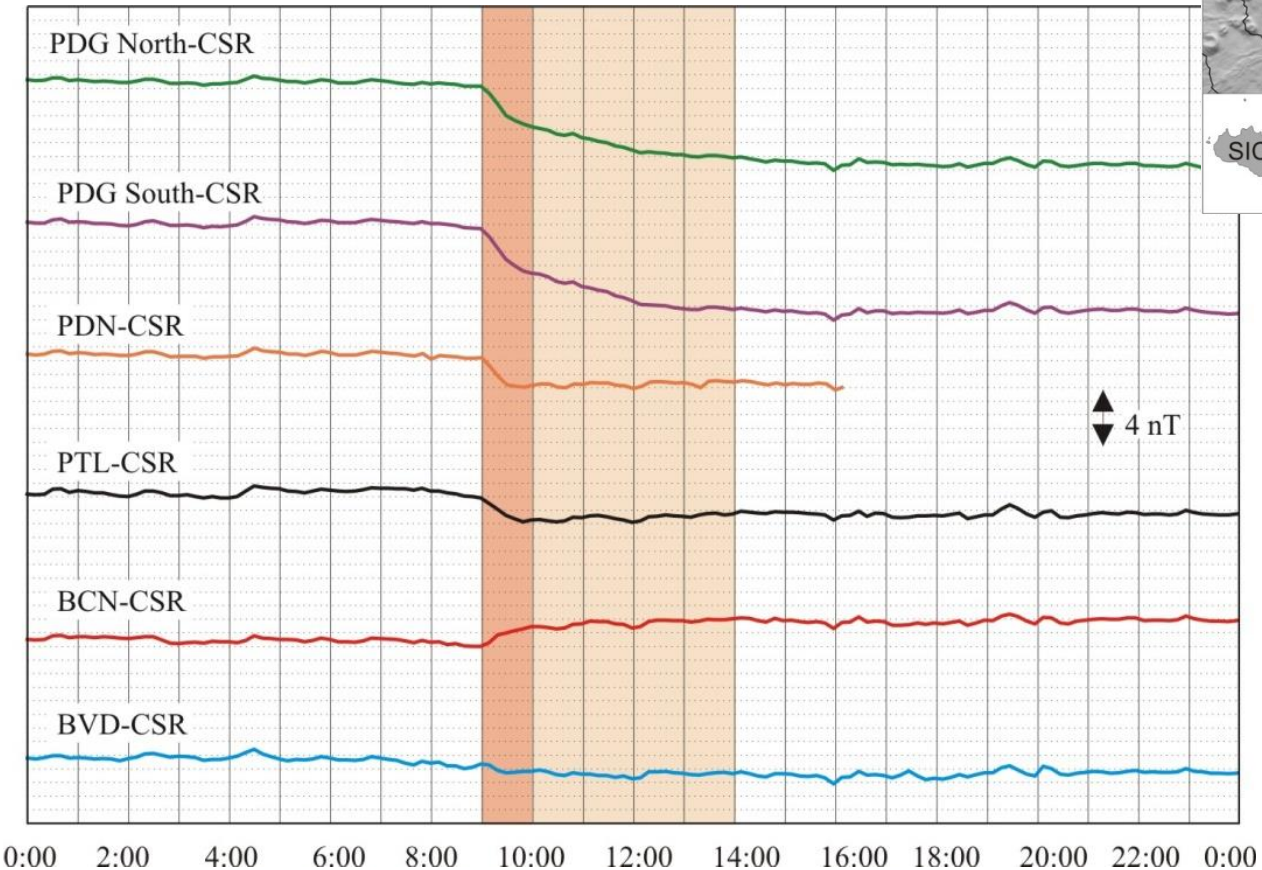

A decrease in the rate of magnetic variations was observed from 10:00 to 14:00 GMT during which a fall in the earthquake rate was observed. After the seismic swarm ended, no further magnetic variations were detected at all stations.

Osservatorio Etneo

Fracture field

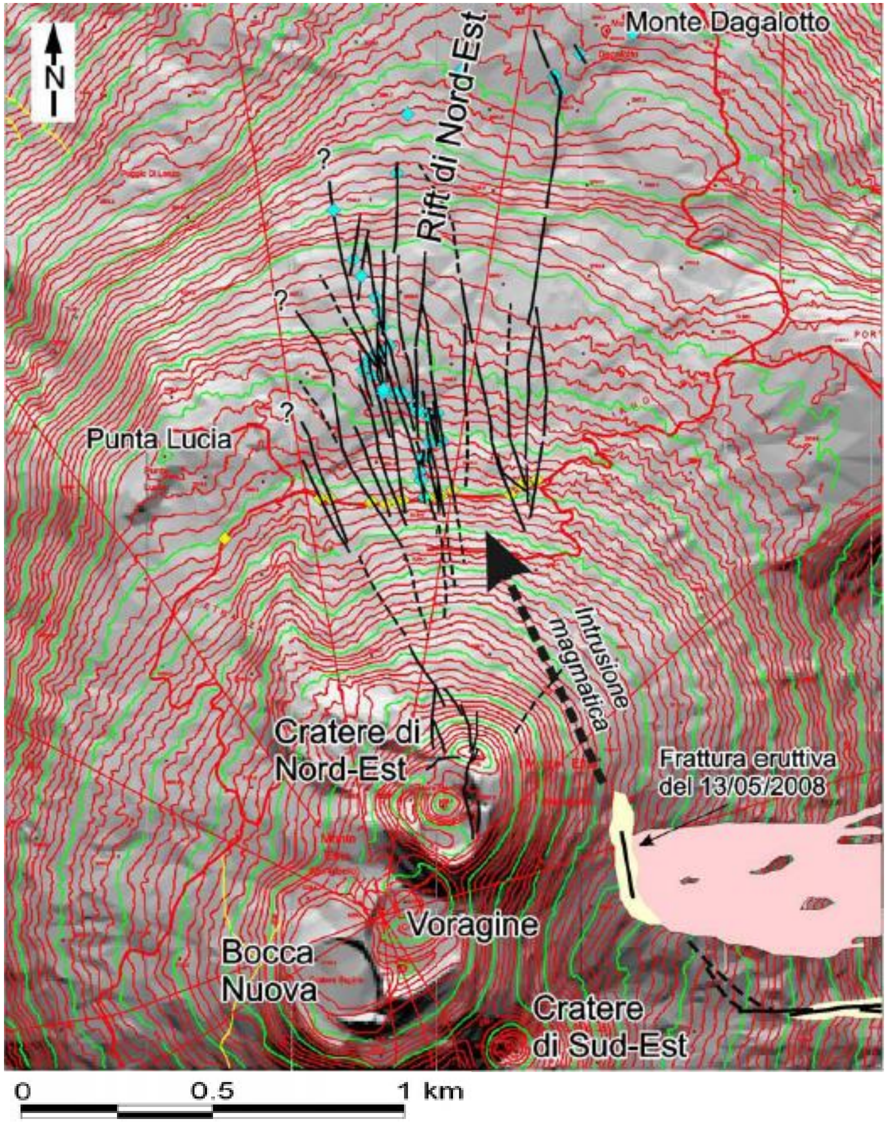

The N170E fracture field in the Northwestern flank of Etna (Gianni Lanzafame, INGV Report, 19 May 2008).
The fracture field, which remained dry extended from the base of the North-East crater for 2000 m along the NNW-SSE direction (Marco Neri, INGV Report, 22 May 2008).

Integrated Magnetic and Deformation Model

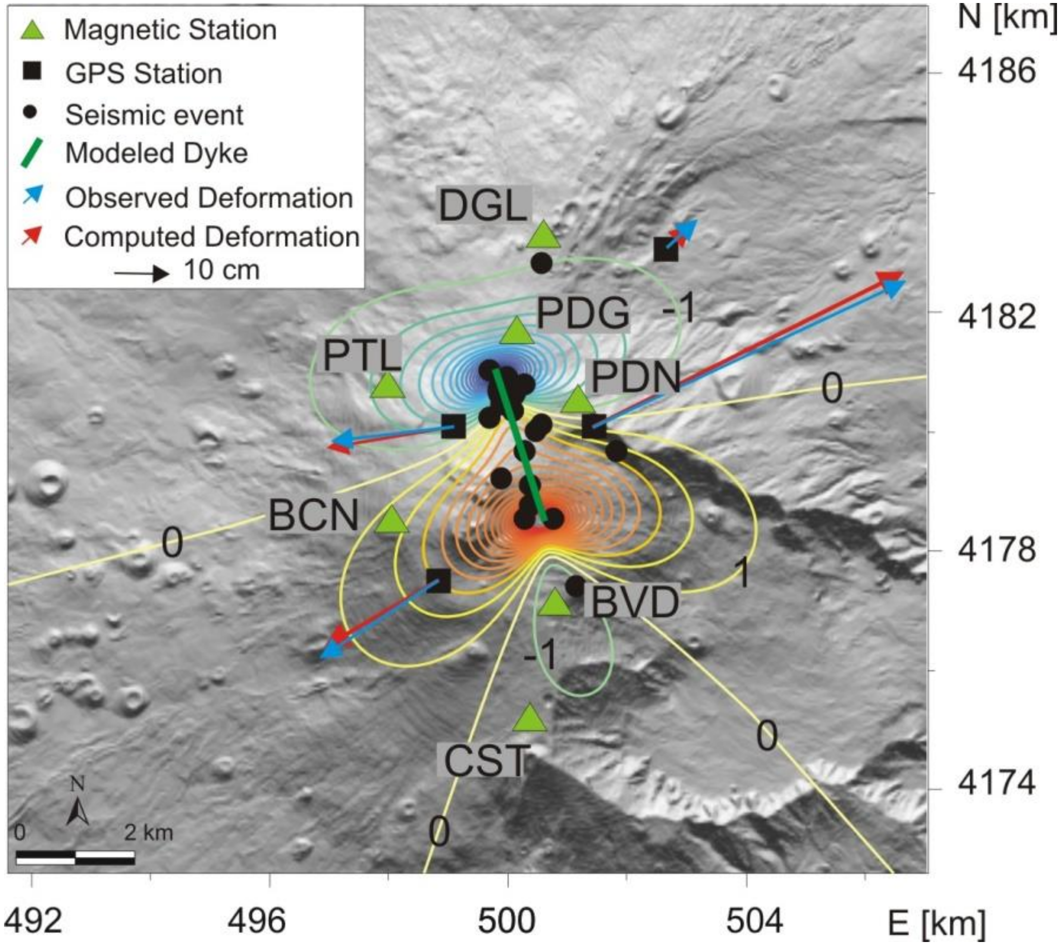

Magneto-elastic medium properties

Magnetization: 4 A/m
Inclination: 53.0°
Declination: 2°
Sensitivity: 10^{-4} bar^{-1}
Rigidity: 16 GPa

Model Parameters	Value
Depth	250 m
Opening	2 m
Width	2 km
Length	2.5 km
X center	4179 km
Y center	500.6 km
Strike	-20°
Slip	80°

The estimated intrusive dike, which explains the observed magnetic data, engenders a deformation pattern [Okada, 1992] that well fits the ground deformation recorded by the continuous GPS network operating on Mt Etna.

Napoli et al., 2008

3D FEM Model

ANALYTICAL MODEL

NUMERICAL MODEL

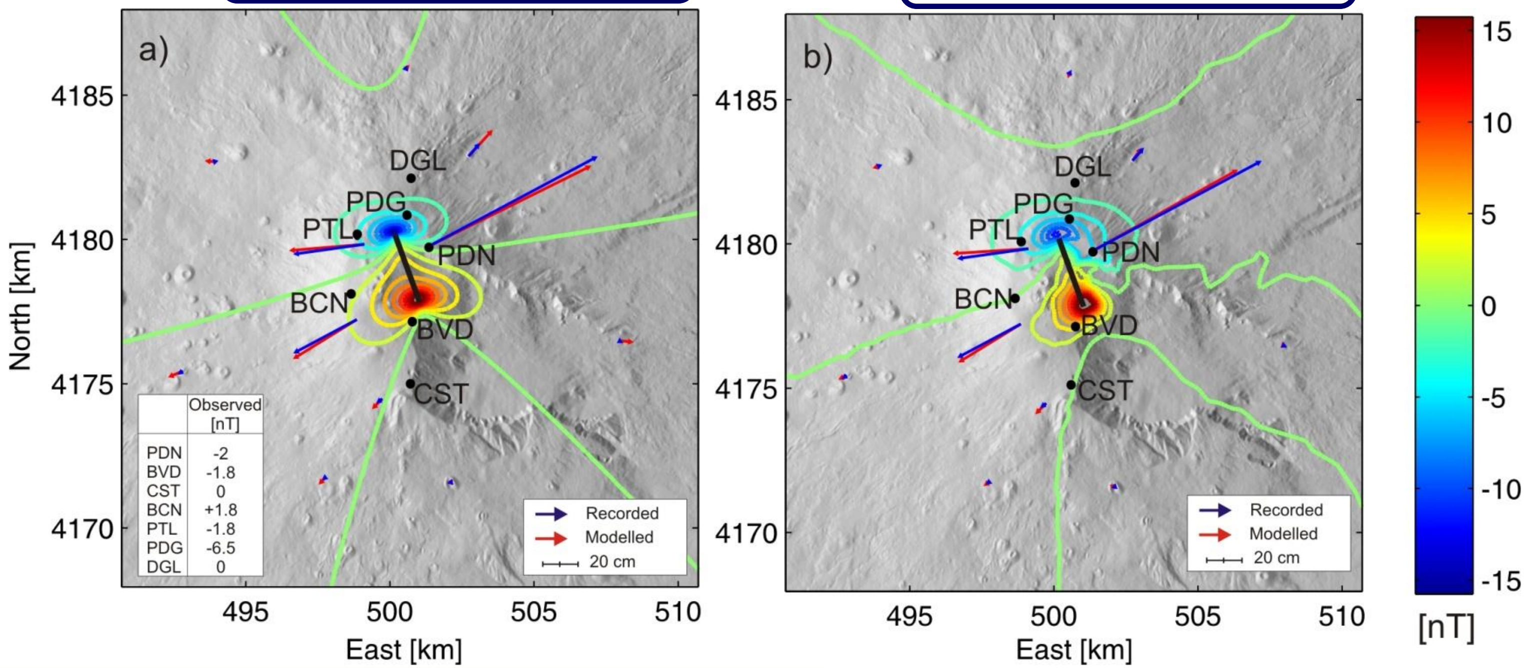

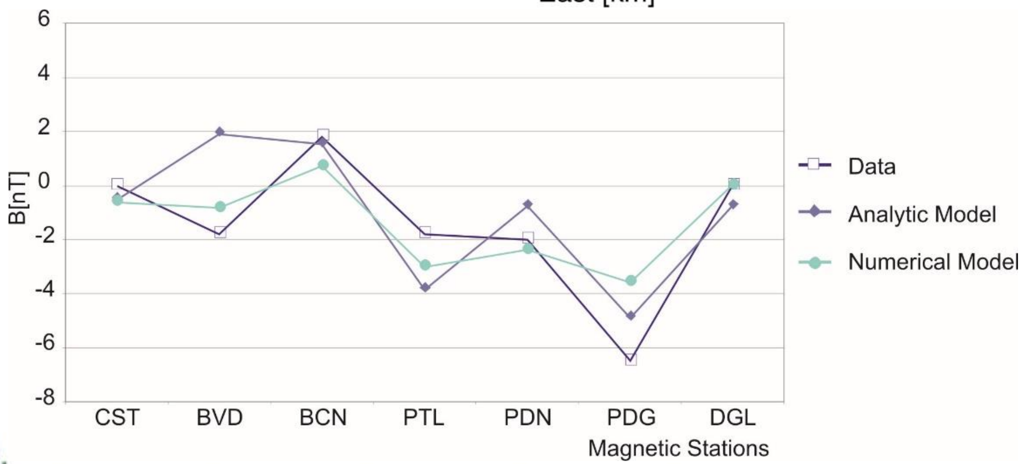

Data misfit

	Analytic Model	Numerical Model
Magnetic	255	150
Horizontal deformation	426	405
Vertical deformation	609	350

Osservatorio Etneo

Gravity Changes

The expected total gravity change reaches an amplitude of about 70 μGal. The anomaly extends about 3-4 km from magma intrusion and does not show significant changes at the gravity benchmarks.

$$\Delta\rho(x,y,z) = \underbrace{\delta\rho_1}_{g_1} - \underbrace{\mathbf{u}\cdot\nabla\rho_0}_{g_3} - \underbrace{\rho_0\nabla\cdot\mathbf{u}}_{g_2}$$

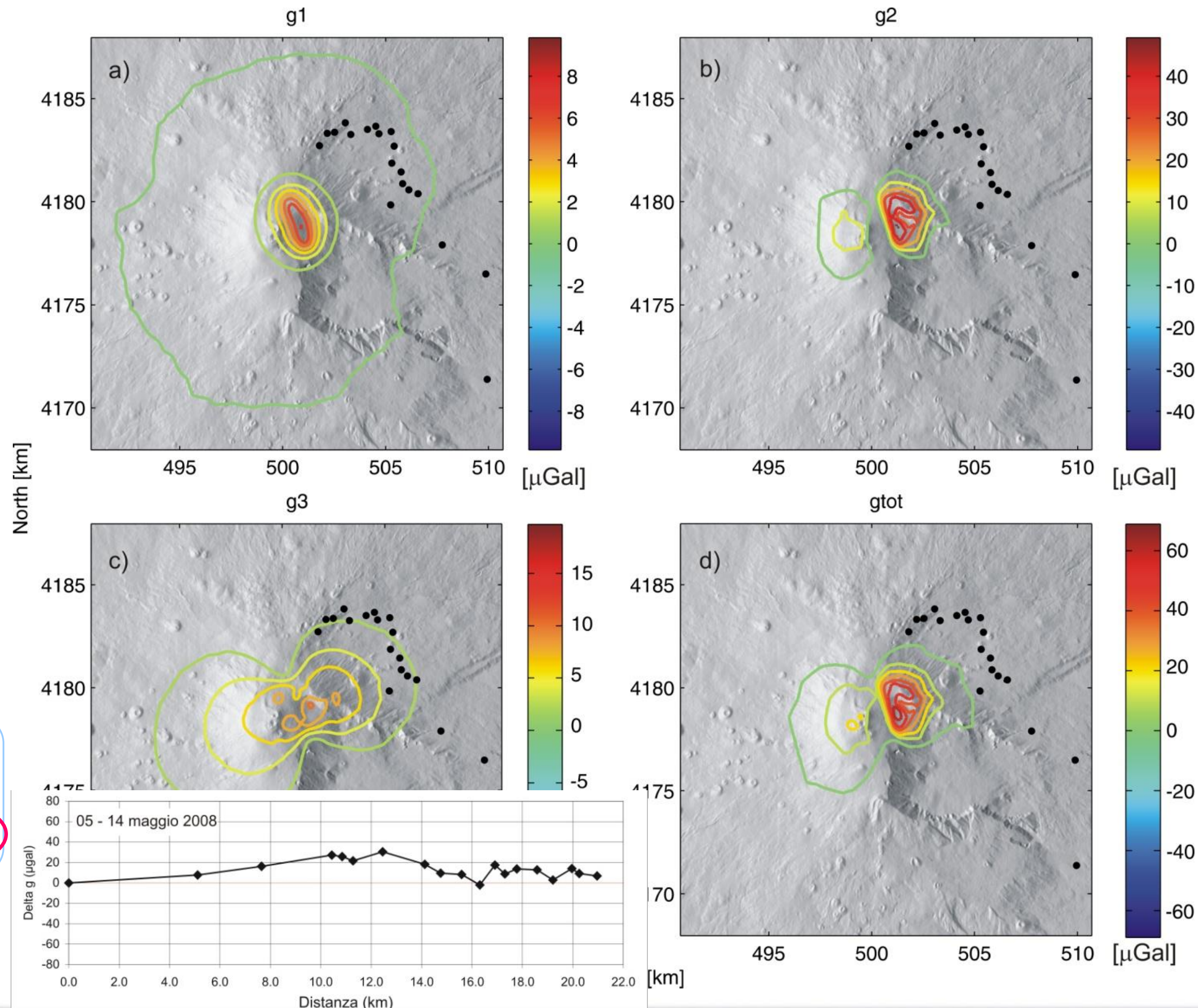

Osservatorio Etneo

DInSAR data

We investigate more complex and realistic dike model from InSAR data rather than simple uniform opening models constrained by few geophysical data from ground based stations. InSAR data provided high spatial resolution deformation pattern. The DInSAR and GPS data correlate with each other. Therefore, we can reasonably assume the DInSAR data reflect mainly the co-intrusive deformation source

Ascending Interferogram (26/03/2008 – 04/06/2008)

Descending Interferogram (07/05/2008 – 16/07/2008)

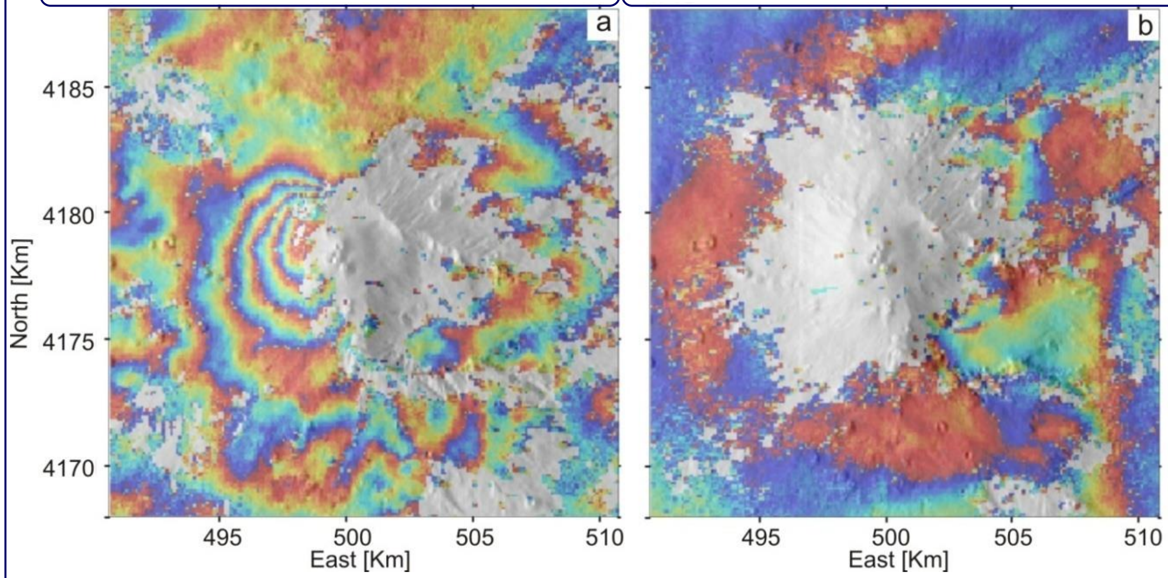

Multiparametric Geophysical Model

We investigate more complex dike model exploiting also InSAR data rather than simple uniform opening models constrained by few geophysical data from ground based stations. InSAR data provided high spatial resolution deformation pattern. The simulated descending interferogram from the distributed opening model enhances the fringes gradient and resemble quite well the overall feature of the observed deformation pattern.

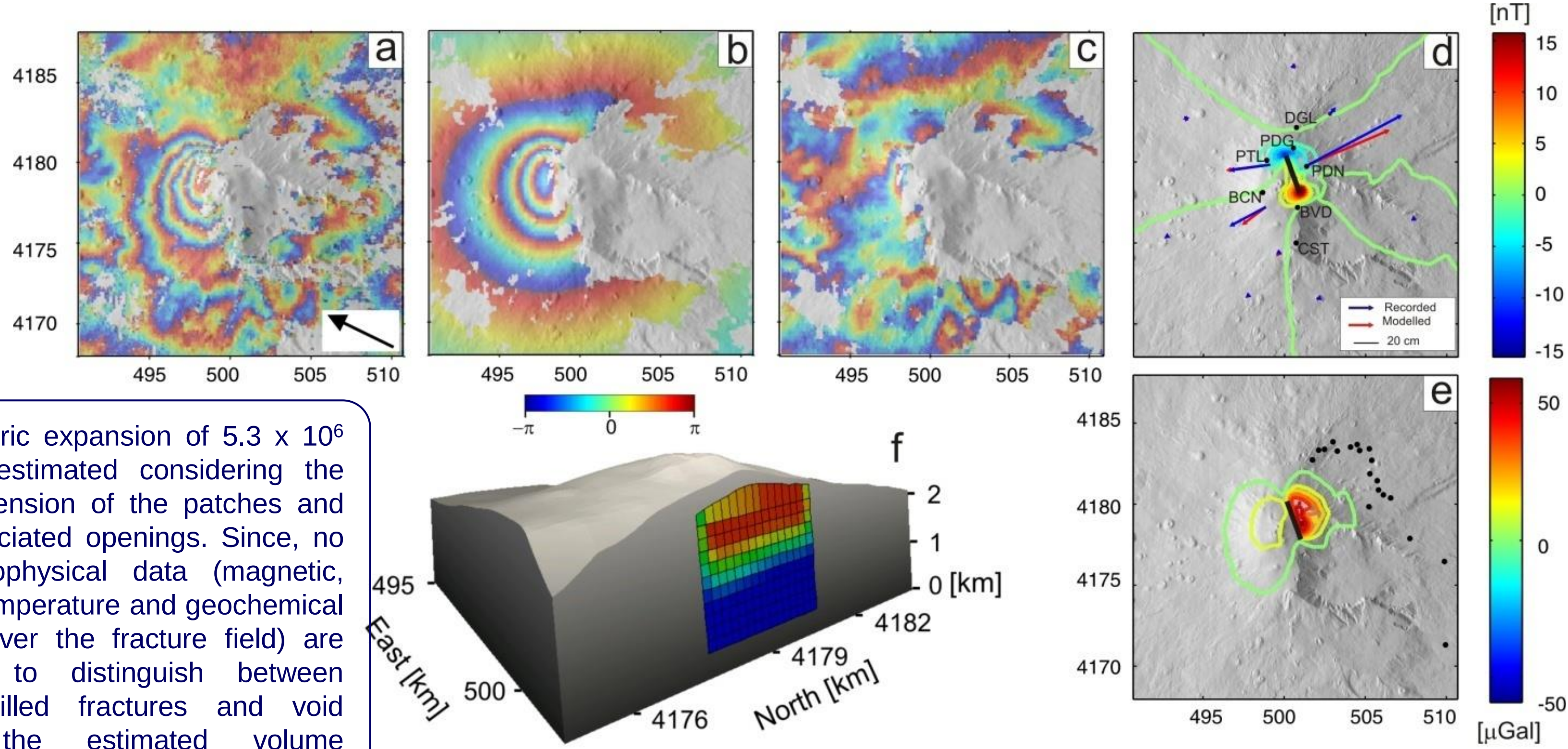

A volumetric expansion of 5.3 x 10^6 m^3 was estimated considering the areal dimension of the patches and their associated openings. Since, no other geophysical data (magnetic, gravity, temperature and geochemical surveys over the fracture field) are available to distinguish between magma filled fractures and void cracks, the estimated volume represents only the upper bound of the intruded magma.

Hydro-Geophysical Model

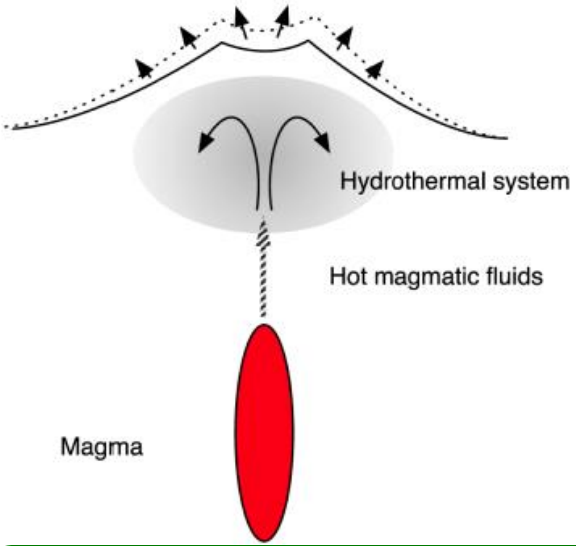

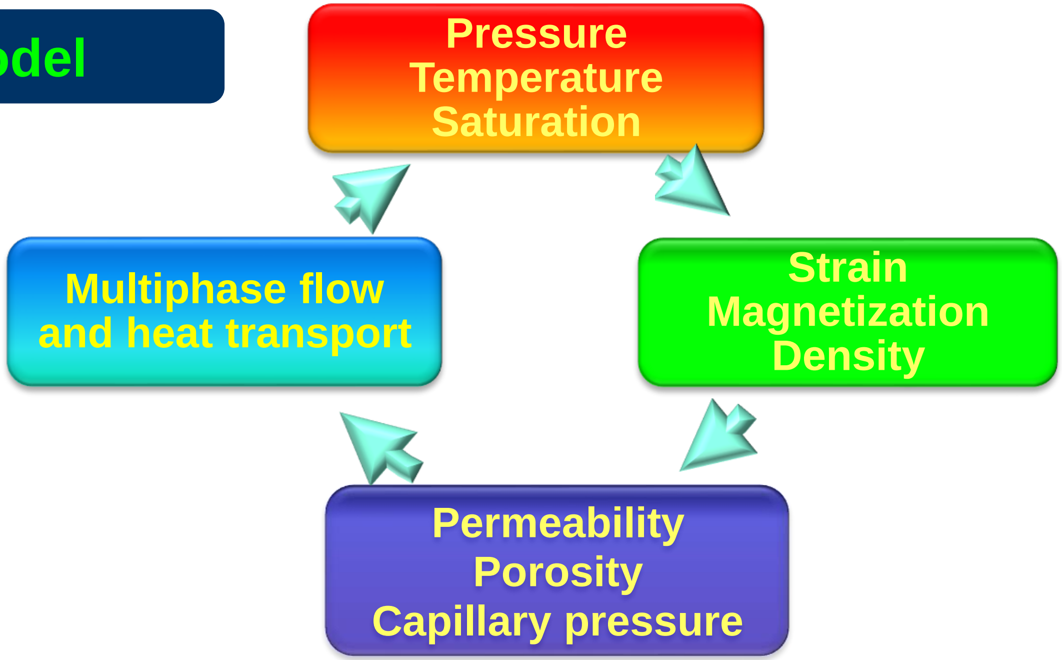

flow /heat transport

$$\frac{\partial(\phi\rho)}{\partial t} - \nabla\cdot\left(\frac{\rho k}{\mu}\left(\nabla p + \rho\mathbf{g}\right)\right) - R_m = 0$$

$$\frac{\partial(\phi\rho h + (1-\phi)\rho_r h_r)}{\partial t} - \nabla\cdot\left(\frac{\rho k h}{\mu}\left(\nabla p + \rho\mathbf{g}\right)\right) - \nabla\cdot(K\nabla T) - R_h = 0$$

deformation

$$\nabla\cdot\left(\mu\left(\nabla\mathbf{u} + (\nabla\mathbf{u})^T\right)\right) + \nabla(\lambda\nabla\cdot\mathbf{u}) - \nabla(p - p_0) - \frac{2G(1+\nu)\alpha}{3(1-2\nu)}\nabla(T - T_0) = 0$$

gravity

$$\nabla^2\phi_g = -4\pi G\Delta\rho \qquad \Delta\rho = \phi(\rho_f S + \rho_g(1-S))$$

Piezomagnetic effect

$$\nabla^2\phi_m = 4\pi\nabla\cdot\mathbf{J}, \quad J_{kl} = J_k^0\beta\mu\left[\frac{3}{2}\left(\frac{\partial u_k}{\partial x_l} + \frac{\partial u_l}{\partial x_k}\right) - \delta_{kl}\nabla\cdot\mathbf{u}\right]$$

Hydro-geophysical Simulations

An hydro-geophysical model has been developed based on thermo-poroelasticity theory, which describes the response of a porous medium to hot fluid migration. The model evaluates the deformation, gravity and thermomagnetic changes due to temperature, pressure and density changes caused by injection of a hot (ca. 350 °C) mixture of water and carbon dioxide.

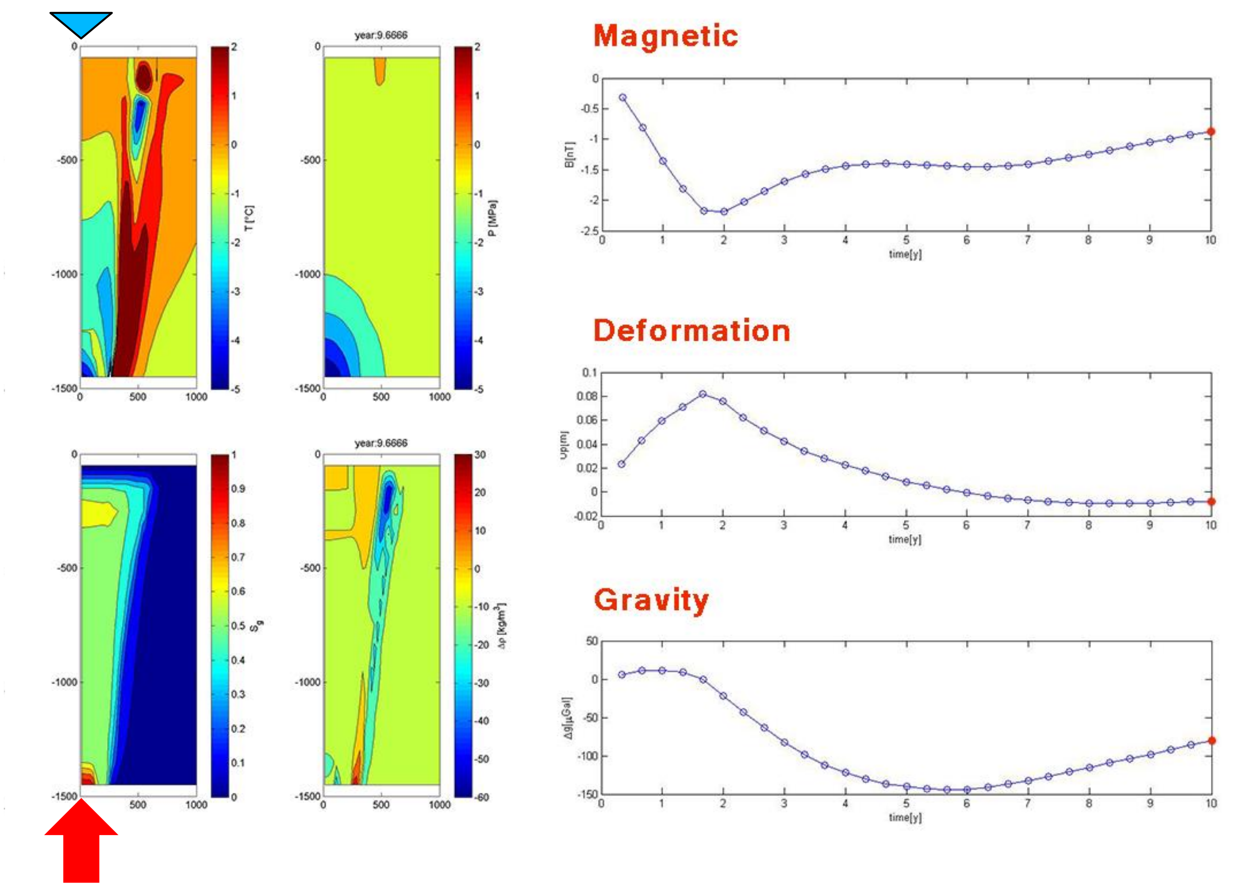

Conclusions

- A coupled numerical problem was solved to estimate ground deformation, gravity and magnetic changes produced by stress redistribution accompanying magma migration within the volcano edifice.

- The integrated numerical procedure was applied to image the magmatic intrusion occurring in the northern flank of Etna during the onset of the 2008 eruption.

- This approach, based on observable data and complemented by physical modeling techniques, makes the step ahead in the volcano hazard assessment and in the understanding of the underlying physics and poses the basis for future developments of scenario forecasting.